Co-expression of the AsCas12a ultra variant, a T7 RNA Polymerase and a cytosine base editor greatly increases transfection and editing rates in *Leishmania* species

Nicole Herrmann May[1], Annika Schmid[1], Elisabeth Meiser[1] and Tom Beneke[1,*]

[1] Department of Cell and Developmental Biology, Biocentre, University of Würzburg, Am Hubland, 97074 Würzburg, Germany

* To whom correspondence should be addressed. Email: tom.beneke@uni-wuerzburg.de

ABSTRACT

The ability to analyse the function of all genes in a genome has obvious appeal. However, this has been challenging in *Leishmania* due to a repetitive genome architecture, limited DNA repair mechanisms and the absence of RNA interference machinery in most species. While our previous introduction of a cytosine base editor (CBE) tool in *Leishmania* showcased the potential for bypassing these limits (Engstler and Beneke (2023)), challenges remained in achieving high transfection efficiencies, overcoming species-specific editing rates, minimizing effects on parasite growth and eliminating competition between deleterious and non-deleterious mutations. Here, we present an optimized approach to address these limitations. Firstly, we identified a T7 RNAP promoter variant that ensures high editing rates across *Leishmania* species without adversely affecting parasite growth. Secondly, we adjusted the scoring of CBE single-guide RNAs (sgRNAs) to prioritize those ensuring STOP codon generation. Thirdly, we developed a triple-expression construct enabling the integration of CBE sgRNA expression cassettes into a *Leishmania* safe harbor locus via AsCas12a ultra-mediated DNA double-strand breaks. This facilitates the generation of stable CBE sgRNA expression cell lines and increases transfection rates by ~400-fold, resulting in up to one transfectant per 70 transfected cells. Lastly, we show how the co-expression of AsCas12a ultra, T7 RNAP and CBE can be utilized for hybrid CRISPR gene replacement and base editing approaches in the same cell line. Overall, we believe that these improvements will broaden the range of possible gene editing applications in *Leishmania* species and will enable a variety of loss-of-function screens in the future.

INTRODUCTION

CRISPR/Cas9 gene editing has greatly improved loss-of-function experiments in *Leishmania*, and bar-seq screens have facilitated the functional dissection of large gene cohorts (Baker et al., 2021; Beneke et al., 2019; Beneke and Gluenz, 2019; Beneke and Gluenz, 2020; Beneke et al., 2017; Burge et al., 2020; Damianou et al., 2020). However, the applications of bar-seq screens are limited, and it remains difficult to target the vast *Leishmania* repertoire of repetitive genetic elements by gene replacement approaches. In addition, *Leishmania* parasites lack crucial components of the non-homologous DNA end joining (NHEJ) pathway (Passos-Silva et al., 2010; Zhang et al., 2022). As a result, CRISPR-induced DNA double-strand breaks (DSB) lead to unpredictable DNA deletions, increased cell death during DNA repair failures, prolonged repair times and generally low editing rates (Zhang et al., 2017; Zhang and Matlashewski, 2015; Zhang and Matlashewski, 2019; Zhang et al., 2022). Without other means of selection, such as the selection of drug resistance-associated edits, this complicates further the targeting of dispersed multi-copy genes and applications of pooled CRISPR transfection formats. While RNA interference (RNAi) could offer an alternative (de Paiva et al., 2015; Lye et al., 2022), its use is confined to species within the *Viannia* subgenus, restricting its applicability in the majority of *Leishmania* species (Lye et al., 2010; Ullu et al., 2004).

We have recently shown how the use of the hyBE4max cytosine base editor (CBE) (Zhang et al., 2020) could potentially overcome these limitations. We demonstrated how the conversion of cytosine to thymine, and thereby the introduction of STOP codons, enables the functional disruption of single- and multi-copy genes in *Leishmania* species without requiring DSB, homologous recombination (HR), the additional use of donor DNA, or isolation of clones (Engstler and Beneke, 2023). Importantly, we presented how this method can be used to identify essential genes in pooled loss-of-function screens via the delivery of plasmid libraries, thereby providing a proof-of-principle experiment for how large-scale pooled CRISPR transfection fitness screens could be carried out in *Leishmania*. However, we also highlighted the need for additional improvements of our method (Engstler and Beneke, 2023).

For example, since we used a ribosomal promoter derived from *L. donovani* for expression of the CBE and single guide RNA (sgRNA), editing efficiencies varied greatly between species, and for some *Leishmania* parasites, sufficient editing could be only achieved after weeks in culture. Our attempts to use different promoters, such as the T7 RNA Polymerase (RNAP) promoter were unsuccessful, as their employment for CBE sgRNA expression resulted in strong growth defects. Furthermore, the transfection of pooled plasmid libraries led to combinatorial knockout effects, with about 38% of all transfectants harbouring more than one CBE-sgRNA expression plasmid. In addition, the transfection efficiency of plasmid pools was generally low, yielding only ~1 transfectant out of 30,000 transfected cells. To compensate for combinatorial effects and the relatively low transfection rate, a large number of cells would need to be transfected to enable large-scale pooled CRISPR transfection screens. Lastly, we noticed that non-deleterious mutations within the CBE editing window can become dominant over desired mutations, especially when targeting essential or growth-affecting genes.

66 Here, we aimed to develop our base editing approach further and deliver needed improvements. We
67 show how we have identified a T7 RNAP promoter variant that enables stable expression of CBE
68 sgRNAs and results in high editing rates within a short period of time without having significant effects
69 on parasite growth. In addition, we present a construct that allows to express not only T7 RNAP and
70 the hyBE4max CBE but also a highly efficient variant of a Cas12a nuclease derived from
71 *Acidaminococcus sp.* (AsCas12a ultra (Zhang et al., 2021), formerly AsCpf1). Using AsCas12a ultra-
72 mediated DSBs, we have developed a novel approach to deliver and integrate CBE sgRNA
73 expression cassettes into the *Leishmania* 18S rRNA safe harbor locus (Misslitz et al., 2000; Sorensen
74 et al., 2003). We demonstrate how this has allowed to increase transfection rates by up to 400-fold. In
75 a final optimisation step, we have also improved our CBE sgRNA design and scoring tool
76 www.leishbaseedit.net to select CBE sgRNAs that have fewer possibilities in generating edits that do
77 not result in a STOP codon. We believe that these optimisation steps now enable us to deliver a
78 range of gene editing applications, including large-scale loss-of-function screens, in *Leishmania*
79 species without limitations due to extreme cases of gene copy numbers, aneuploidy and/or lack of
80 RNAi components.

81

RESULTS and DISCUSSION

T7 RNAP promoter variant-driven CBE sgRNA expression reduces toxicity and improves editing efficiency

In our first version of a CBE toolbox for *Leishmania* we utilized a ribosomal promoter derived from *L. donovani* for CBE protein and sgRNA expression. While achieving high editing rates with this single plasmid system (Figure 1A) (Engstler and Beneke, 2023), efficiencies varied greatly among species, requiring for example over 40 days of incubation to reach significant editing in *L. major* parasites. We previously attempted to minimize these species-specific variations by segregating the CBE expression from the CBE sgRNA cassette in a dual construct system and by employing a T7 RNAP promoter for CBE sgRNA expression (Figure 1B). However, upon transfection of CBE sgRNA expression constructs into *L. major* T7 RNAP- and CBE-expressing parasites, the doubling time increased from 7 to about 14 hours, highlighting a significant growth defect through T7 RNAP-driven CBE sgRNA expression. On the contrary, we observed higher editing rates in a shorter period of time compared to our approach with the single plasmid ribosomal promoter system, indicating potential advantages (Engstler and Beneke, 2023).

Here, our first aim was to eliminate this growth defect observed in the dual construct system while maintaining high editing rates. Assuming that the growth defect resulted from excessive CBE sgRNA expression, we wondered whether modifying the T7 RNAP promoter sequence and altering the transcription initiation site could alleviate the observed toxicity. We therefore introduced a variety of CBE sgRNA expression plasmids into our previously established *L. major* cell line, expressing CBE and T7 RNAP from the β-tubulin locus, as well as tdTomato from the 18S rRNA locus (Engstler and Beneke, 2023) (Figure 1B). To drive CBE sgRNA expression, we thereby utilized two T7 RNAP promoter variants (T7 T-10 and T7 G-10), known for their ability to reduce transcription activity in the closely related parasite *Trypanosoma brucei* (Wirtz et al., 1998). We also manipulated the transcription initiation site by altering the number of guanines (either two or one guanines), a factor believed to impact transcription yield (Padmanabhan et al., 2020) (Figure 1C). Additionally, we compared CBE sgRNA expression via T7 RNAP promoters with the ribosomal promoter derived from *L. donovani*, either in a single or dual construct system setup. For our measurements, we transfected CBE sgRNA expression plasmids with two tdTomato-targeting CBE sgRNAs. While the ‘target’ CBE sgRNA was designed to yield an early STOP codon through C to T conversion, the ‘control’ CBE sgRNA was designed to induce a C to T conversion that results in a neutral substitution (codon change but no amino acid change). Following transfection, we then analysed growth rates (Figure 1D) and tdTomato reporter signals (Figure 2E and F). Our aim was to identify the promoter variant with the highest activity and least toxicity.

As anticipated, when utilizing the ribosomal promoter for CBE sgRNA expression, the dual construct system resulted in a more significant reduction of the tdTomato reporter signal compared to the single plasmid system. The complete knockdown of the tdTomato reporter was also achieved using all T7 RNAP promoter variants with the dual construct system. While there were no detectable differences in these knockdown efficiencies (Figure 2E and F), there were notable variations in the growth rates

121 (Figure 1D). Consistent with our prior observations (Engstler and Beneke, 2023), cells transfected
122 with constructs containing the unmodified T7 RNAP promoter sequence (T7 wt GG in Figure 1D)
123 exhibited an almost two-fold increase in doubling time. On the contrary, employing for CBE sgRNA
124 expression the T7 T10 GG, T7 G10 GG and ribosomal promoter resulted in no significant growth rate
125 increase. The doubling times here ranged from 7.5 to 8.1 hours. While this aligned with
126 measurements obtained for cells transfected with our single plasmid system (Figure 1D), the
127 complete knockdown of the tdTomato reporter was much more rapid using any dual construct system
128 (Figure 1E). Specifically, the complete depletion of the tdTomato reporter signal was achieved in just
129 seven days (Figure 1E) compared to 33 days when using the same CBE sgRNA in *L. major* parasites
130 previously (Engstler and Beneke, 2023). This demonstrates a major improvement in our method to
131 generate loss-of-function mutants in non-clonal populations.

132 **DSBs introduced by AsCas12a ultra increase integration rates of donor DNA constructs**

133 Having successfully improved editing efficiencies, while at the same time reducing the toxicity of CBE
134 sgRNA expression and targeting, we next attempted to increase transfection rates of the CBE sgRNA
135 expression constructs. Previously, we have shown that ~30,000 *L. mexicana* wildtype cells need to be
136 transfected with our single plasmid system (Figure 1A) to obtain one transfectant (Engstler and
137 Beneke, 2023). Since genomic dropout screens need to be performed at a high representation of
138 about 500 cells per sgRNA construct (Sanjana et al., 2014; Yau and Rana, 2018), this relatively low
139 transfection rate would make any large-scale screen challenging. In addition, we wanted to enable
140 screening of base editor libraries over long periods and in complex environments, such as *in vivo*
141 experiments, without risking that parasites would lose their CBE sgRNA plasmid, vary their plasmid
142 copy number or transfer plasmids between cells. Therefore, we wanted to integrate CBE sgRNA
143 expression constructs into a safe harbor locus. Strategies to increase transfection rates and stably
144 integrate expression cassettes by homologous recombination have been previously developed in *T.*
145 *brucei*. Here, the use of an I-SceI mega- (Glover and Horn, 2009) or zinc finger- (Schumann et al.,
146 2017) nuclease-induced DSB at a safe harbor locus has been shown to increase the transfection
147 efficiency for the integration of RNAi expression constructs significantly. In combination with improved
148 transfection protocols (Burkard et al., 2007; Glover and Horn, 2009), this has enabled RNAi loss-of-
149 function screens on a genome-wide scale (Glover et al., 2015; Horn, 2022; Schumann Burkard et al.,
150 2011). Alternatively, it has been shown in *Leishmania* that CRISPR/Cas9-induced DSBs can increase
151 the rate of correct donor DNA integration, regardless of homology flank length (Beneke et al., 2017).

152 To develop a strategy for stable integration of CBE sgRNA expression constructs in *Leishmania*
153 species, we decided to employ a Cas12a nuclease variant from *Acidaminococcus* species.
154 Specifically, we generated an expression construct (pTB107) to co-express in *Leishmania* the
155 AsCas12a ultra variant (Zhang et al., 2021), a T7 RNAP and the hyBE4max CBE (Engstler and
156 Beneke, 2023) (Figure 2A). The use of AsCas12a ultra had several advantages compared to other
157 approaches mentioned above. Firstly, compared to the use of I-SceI meganuclease (Glover and Horn,
158 2009), it allowed us to select any TTTV-PAM containing locus of interest to insert our CBE sgRNA
159 expression construct, simply by just changing the Cas12a crRNA sequence. Secondly, Cas12a

160 editing – just like any CRISPR strategy – is much simpler to design than a zinc-finger nuclease
161 (Schumann et al., 2017) or TALENs approach. Thirdly, compared to a functional SpCas9 nuclease,
162 there was no risk of interference between the Cas9 base editor and Cas9 nuclease sgRNAs. Finally,
163 since AsCas12a has an intrinsic RNase activity that allows processing of its own crRNA array (Paul
164 and Montoya, 2020), multiplexing of guide sequences is possible, which could expand the scope of
165 standard CRISPR knockin and knockout approaches in *Leishmania* in future studies. Ultimately, we
166 figured that the co-expression of the AsCas12a ultra nuclease, a T7 RNAP and the CBE would
167 generate a hybrid gene editing toolbox that has many possible applications.

168 To introduce AsCas12a-mediated DSBs, we decided to adapt the LeishGEdit approach, which was
169 previously developed for delivering Cas9 sgRNAs (Beneke and Gluenz, 2019; Beneke et al., 2017).
170 Specifically, we designed two overlapping oligos capable of being mutually amplified, generating a
171 Cas12a crRNA template DNA (Figure 2B). This resulting template featured an unmodified T7 RNAP
172 promoter sequence, facilitating the *in vivo* transcription of the Cas12a crRNA. To ensure high binding
173 affinity of AsCas12a with its Cas12a crRNA, we used an optimized direct repeat (DR) from DeWeirdt
174 et al. (2021). Subsequently, this enabled AsCas12a ultra-mediated DSBs for donor DNA integration.
175 To test this approach, we utilized a donor DNA construct containing mNeonGreen (mNG) as a
176 reporter and blasticidin as a resistance marker, allowing for a relatively straightforward assessment of
177 integration accuracy and transfection rate (Figure 2A). Additionally, we varied the length of homology
178 flanks to investigate whether Cas12a-mediated integration of donor DNA remained independent of
179 homology flank length, as previously observed with Cas9 (Beneke et al., 2017). Using homology
180 flanks routinely used for integration into the 18S rRNA safe harbor locus of various *Leishmania*
181 species (Misslitz et al., 2000; Sorensen et al., 2003), we then designed one Cas12a crRNA targeting
182 the 200bp region between both homology regions (Figure 2 S1A). To evaluate if Cas12a could
183 enhance the transfection rate, we compared transfections of these reporter constructs with and
184 without the addition of Cas12a crRNA.

185 Like findings with Cas9, we observed that Cas12a-induced DSBs in *L. mexicana* increased the rate of
186 correct donor DNA integration, irrespective of homology flank length. Integration of reporter constructs
187 with 600 nt homology flanks showed no difference in reporter signal (Figure 2C), but the addition of
188 Cas12a crRNA boosted transfection efficiency by approximately 25-fold when assessing blasticidin-
189 resistance rates (Figure 2D). When reducing homology flank length to 60 nt, we observed no impact
190 on the reporter signal or transfection rate when Cas12a crRNA was present during transfections.
191 However, in the absence of Cas12a crRNA, no transfectants were obtained, confirming that
192 homologous recombination of the reporter is only independent of homology flank length if a Cas12a-
193 mediated DSB has occurred. Further reducing the homology flank length to 30 nt did not significantly
194 decrease transfection efficiency, but the percentage of mNG positive cells decreased from ~99% in all
195 other samples to 96.7% (Figure 2C). Conversely, Sanger sequencing off all integration sites indicated
196 flawless recombination for all constructs (Figure 2 S1A, B and C). Interestingly, diversity in the
197 reporter signal was also noted when transfecting the mNG construct as an episome (Figure 2C),
198 possibly pointing towards plasmid copy number variants between transfected cells. In addition,

199 episomal transfections using the same number of DNA molecules resulted in a significantly lower
200 number of transfectants (Figure 2D), concluding the advantages of integrating expression constructs
201 via Cas12a-mediated DSBs.

202 We then wondered whether employing different Cas12a crRNAs could enhance the transfection
203 efficiency even further. Three additional Cas12a crRNAs within the 18S rRNA SSU locus were
204 selected for testing (Figure 2 S1D). In addition, we sought to examine the integration into a "landing-
205 pad", such as a previously introduced resistance marker. We expected that this would further increase
206 the accuracy and efficiency of the transfection. We therefore decided to test our system in a
207 tdTomato-expressing *L. mexicana* cell line (Engstler and Beneke, 2023) and designed two Cas12a
208 crRNAs to integrate mNG-blasticidin donor DNA constructs within their neomycin-resistance marker
209 (Figure 2 S1D). Given that 60 nt homology flank length was sufficient for accurate and efficient
210 integration of donor DNA (Figure 2C and D), we decided to test all six Cas12a crRNAs in combination
211 with donor DNA constructs containing 60nt homology flanks. This meant that homology flanks could
212 be easily adapted through long-primer PCR without the need for bacterial cloning.

213 Across all six Cas12a crRNAs tested, no significant changes in the proportion of mNG-expressing
214 cells were observed (Figure 2E). However, there was a substantial variation in the rate of blasticidin-
215 resistant cells, indicative of Cas12a crRNA efficiency (Figure 2F). For Cas12a crRNA-1, we confirmed
216 our previous results, yielding one transfectant per ~8,500 transfected cells. However, other Cas12a
217 crRNAs, particularly Cas12a crRNA-4, performed significantly better, resulting in one transfectant out
218 of approximately 2,300 transfected cells. Interestingly, despite being only 44bp upstream of Cas12a
219 crRNA-4, Cas12a crRNA-3 exhibited a 500-fold lower integration efficiency. Surprisingly, both
220 neomycin-targeting Cas12a crRNAs were less efficient than the majority of 18S rRNA SSU locus-
221 targeting guides (Figure 2F). Given the exceptional efficiency of Cas12a crRNA-4, we verified the
222 integration of donor DNA at its site through Sanger sequencing, confirming flawless integration
223 (Figure 2 S1D, E, and F).

224 **Integration of CBE sgRNA expression cassettes via AsCas12a ultra-introduced DSBs increase**
225 **editing rates**

226 After successfully validating our here developed AsCas12a ultra-mediated integration system, we
227 then decided to combine our Cas12a knock-in system with our optimized CBE sgRNA expression
228 cassette (Figure 3A). For this purpose, we developed two CBE sgRNA expression plasmids, namely
229 pTB104 and pTB105, each incorporating a puromycin-resistance marker and the most effective T7
230 RNAP promoter variant (T7 T10 GG) for CBE sgRNA expression (as identified in assays above;
231 Figure 1C, D and E). While pTB104 featured 350 nt homology flanks adjacent to the neomycin-
232 targeting Cas12a crRNA-6, pTB105 included 350 nt homology flanks adjacent to our best-performing
233 Cas12a crRNA-4, targeting the 18S rRNA SSU locus. This design allowed for the integration of both
234 CBE sgRNA expression cassettes with and without the addition of Cas12a crRNAs. To assess if such
235 a system could effectively generate a functional null mutant through cytosine-to-thymine conversion,
236 we chose to target tdTomato again and tested a tdTomato-targeting CBE sgRNA in *L. donovani*, *L.*
237 *mexicana*, and *L. major*. Parasites expressed tdTomato, along with the CBE, Cas12a ultra, and T7

238 RNAP (Figure 3A). Additionally, we investigated whether the efficiency of the tdTomato knockdown
239 would be influenced by how the CBE sgRNA expression cassette was integrated. We therefore
240 compared Cas12a crRNA-4 and 6 in combination with 60 and 350 nt homology flanks.

241 Strikingly, we observed a complete depletion of the tdTomato signal just 7 days post transfection in all
242 tested species when integrating CBE sgRNA expression cassettes into the 18S rRNA SSU locus.
243 This occurred irrespective of homology flank length. However, integrating cassettes into the neomycin
244 resistance marker resulted in only partial tdTomato knockdowns in *L. major* and *L. donovani*, while a
245 complete knockdown could again be achieved in *L. mexicana*. Although we have not further
246 investigated the cause for this, we assume that either the low efficiency of Cas12a crRNA-6 or the
247 number of tdTomato-neomycin-expression cassettes caused this discrepancy. Overall, this highlights
248 that integrating CBE sgRNA expression cassettes into the 18S rRNA SSU locus using Cas12a
249 crRNA-4 in combination with plasmid pTB105 would yield the highest CBE sgRNA editing efficiency.
250 We therefore tested next the transfection rate of CBE sgRNA expression cassettes using Cas12a
251 crRNA-4 for integration in *L. mexicana*, *L. major* and *L. donovani*. We reached high transfection
252 efficiencies, yielding up to one transfectant out of ~470 transfected *Leishmania* parasites, with *L.*
253 *donovani* being the most and *L. major* being the least efficient (Figure 3C, left panel).

254 We then wondered whether we could increase the transfection efficiency even further by using the
255 Lonza Nucleofector technology. Previous studies in *T. brucei* demonstrated that the improved
256 transfection rate achieved through I-SceI meganuclease-mediated cleavage could be further
257 increased when combined with the Lonza Nucleofector technology, resulting in up to one transfectant
258 per 100 transfected cells (Glover and Horn, 2009). Considering this, we explored whether this
259 approach would be as effective in *Leishmania* parasites. We therefore conducted a site-by-site
260 comparison of the transfection efficiency between the Lonza Nucleofector Basic Parasite kit and the
261 *Trypanosoma*-optimized buffer (Tb-BSF buffer, see method section for further details) (Schumann
262 Burkard et al., 2011), both in combination with an Amaxa Nucleofector 2b electroporator. To increase
263 the number of parasites per transfection even further, we compared our standard transfection protocol
264 using 5×10^6 cells per transfection with up-scaled transfection formats involving 1×10^8 cells and
265 2.5×10^8 cells per electroporation. Testing these conditions in *L. mexicana*, we confirmed that the
266 Lonza Nucleofector technology could indeed boost transfection efficiency by an additional 20-fold
267 (Figure 3C, right panel). When transfecting 1×10^8 cells per transfection with 10 µg of PacI-linearized
268 pTB105 plasmid DNA, we achieved up to one transfectant out of 70 transfected cells (Figure 3C, right
269 panel). This represents a more than 400-fold increase in transfection efficiency compared to our
270 previous rates (Engstler and Beneke, 2023). Moreover, it demonstrates that a CBE sgRNA library with
271 40,000 constructs could be transfected at a representation rate of 500-fold using just 20×10^8 cells
272 across 20 transfection cuvettes. Ensuring a 500-fold library representation represents a substantial
273 improvement compared to previous RNAi screens in *T. brucei*, where screens typically achieved
274 about 5-9-fold library representation (Glover et al., 2015; Horn, 2022; Morris et al., 2002; Schumann
275 Burkard et al., 2011). This high representation rate is considered crucial for large-scale dropout
276 screens, as it can affect hit identification by minimizing variations between replicates. However, it's

277 worth noting that drug resistance screens can also be conducted at much lower coverage (Sanjana et
278 al., 2014; Yau and Rana, 2018).

279 While the significantly enhanced transfection rates are a central aspect of our improved base editing
280 method presented here, it is crucial to emphasize that these improvements were achieved without
281 impacting parasite growth. Through an assessment of doubling times in transfected and parental cell
282 lines, we confirmed that the expression of CBE, T7 RNAP, AsCas12a ultra, and the CBE sgRNA had
283 minimal or no impact on parasite growth across all three species (Figure 3D). This marks a substantial
284 improvement, considering that the expression of CBE and/or CBE sgRNA in our first toolbox version,
285 using the pLdCH-hyBEmax plasmid, could lead to significant growth defects in some *Leishmania*
286 species (Engstler and Beneke, 2023).

287 Having established this optimised system, we next decided to target PF16, a gene encoding a central
288 pair protein of the axoneme that has been demonstrated to be essential for *Leishmania* flagellar
289 motility (Beneke et al., 2017; Engstler and Beneke, 2023; Martel et al., 2017). For our test, we chose
290 to utilize a previously employed PF16-targeting CBE sgRNA, namely PF16-3. This specific CBE
291 sgRNA induces paralysis in *Leishmania* parasites by introducing a thymidine homo-polymer ("TTTTT")
292 within the PF16 coding sequence. While our usual design for CBE sgRNAs aims to introduce STOP
293 codons through cytosine-to-thymine conversion, we selected PF16-3 for this test because its editing
294 activities are known to vary across species (Engstler and Beneke, 2023). In earlier attempts, we had
295 to express CBE sgRNA PF16-3 for 42 days to achieve sufficient editing in *L. major* when using our
296 pLdCH-hyBE4max single vector (Figure 1A) (Engstler and Beneke, 2023). Meanwhile, in *L. donovani*,
297 high editing rates were already achieved 14 days post transfection. Now, we expected that editing
298 rates had improved uniformly across all species.

299 As anticipated, we observed a significant increase in editing activity in *L. major* parasites. Just 14
300 days post transfection, we found that the homo-polymer had been fully introduced when using our T7
301 RNAP promoter-based dual vector system, while no editing could be observed using the ribosomal
302 promoter single vector system at this time point (Figure 4B, *L. major* panel). This was also reflected in
303 the analysis of mutant swimming speed, revealing clear motility defects in respective transfectants
304 (Figure 4A, *L. major* panel).

305 We next proceeded to test our optimized system also in *L. mexicana* and *L. donovani* parasites, once
306 again employing Cas12a for integration of the CBE sgRNA expression construct. However, here we
307 chose to target PF16 in two cell lines: (i) one that possessed the pTB107 construct and a tdTomato
308 reporter, and (ii) one that possessed the pTB107 construct only (WT pTB107). Additionally, we took
309 this opportunity to compare motility and CBE editing rates in cells that had been transfected with
310 Cas12a crRNAs that target the neomycin-resistance marker (Cas12a crRNA-6) and the 18S rRNA
311 SSU locus (Cas12a crRNA-4).

312 Our results clearly showed that just 6 days post transfection, the PF16 target site was fully edited, and
313 the overwhelming majority of all cells were paralyzed in all tested scenarios (Figure 4A and B).

314 However, surprisingly editing slowly reversed in *L. mexicana* cells harboring the pTB107 construct
315 only (Figure 4A and B). Although we decided not to further investigate the reason for this unexpected
316 result, we assumed that it might be caused by a small proportion of cells where the CBE sgRNA
317 expression cassette was incorrectly integrated. Since the PF16 mutation in *L. mexicana* is known to
318 be associated with a mild growth defect (Beneke et al., 2019), PF16-deficient mutants would
319 eventually be outcompeted over time, leading to the reversal of editing rates. But this phenomenon
320 was not observed in any other tested cell line, when comparing editing and motility rates 6 and 16
321 days post transfection. Both tested *L. donovani* cell lines and the tested *L. mexicana* cell line that
322 possessed the pTB107 construct and the tdTomato expression cassette (Figure 4A and B) remained
323 paralyzed over the entire observation time. To confirm that these cells would have no potential ever to
324 reverse their phenotype, we decided to Illumina sequence paralyzed *L. mexicana* PF16 mutants 16
325 days post transfection. Analyzing their sequencing data, we did not find a single read of an unedited
326 PF16 CDS sequence (with approximately 35× genome coverage), confirming that indeed all cells
327 were completely mutated (Figure 4 S1A).

328 **Cas12a-mediated DSB ensures the integration of one CBE sgRNA per *L. mexicana* transfectant**

329 We next wanted to verify how exactly the CBE sgRNA expression cassette had been integrated via
330 Cas12a-mediated DSB in *L. mexicana* cells that possessed the pTB107 construct and the tdTomato
331 reporter. Since the tdTomato expression cassette is just ~400 nt upstream of the Cas12a crRNA-4
332 target sequence, we wondered whether it had come to any obvious interference between the
333 tdTomato and CBE sgRNA expression cassettes. Given the highly repetitive nature of the 18S rRNA
334 SSU locus, we employed Oxford Nanopore Technology (ONT) sequencing to determine the exact
335 integration pattern of both cassettes. For the analysis of sequencing reads, we mapped them against
336 two customized genomes. In the first genome, we assumed that the tdTomato expression cassette
337 was integrated separately from the CBE sgRNA construct, implying that each cassette had integrated
338 on the opposite allele (Figure 4 S1B). In the second genome, we assumed that both cassettes were
339 integrated on the same allele and could be detected on a single ONT read (Figure 4 S1C).

340 Interestingly, we could only map unique ONT reads to the first scenario, where cassettes were
341 assumed to be integrated on separate alleles and present in only one copy in the genome. These
342 ONT reads covered the entire tdTomato or CBE sgRNA expression cassette, as well as sequences
343 adjacent to homology flanks used for integration (Figure 4 S1B and C). To validate our findings, we
344 revisited our Illumina sequencing data and analyzed the coverage of relevant genetic features.
345 Specifically, we normalized all reads to the total number of reads per chromosome and compared the
346 normalized coverage of reads mapped to the CDS of PF16, the CBE sgRNA cassette, the CDS of
347 tdTomato, and the CDS of the neomycin-resistance marker. While we found equal read coverage of
348 PF16-mapped reads and the chromosome harboring PF16, read coverage for the CBE sgRNA
349 cassette, the CDS of tdTomato, and the CDS of the neomycin-resistance marker were approximately
350 half of the read coverage of their harboring chromosome 27 (Figure 4 S1D). This confirmed our
351 hypothesis that indeed the CBE sgRNA expression cassette had only been integrated on one allele,
352 and most likely, this meant that only one CBE sgRNA cassette copy was present per *L. mexicana* cell.

353 This represents a major improvement since, in our previously used single vector system, about 38%
354 of all *L. mexicana* transfectants possessed more than one CBE-sgRNA expression plasmid,
355 potentially causing combinatorial knockout effects. To verify that in our new dual system each cell
356 indeed harboured only one CBE sgRNA, we decided to test if isolated clones from a transfected
357 library would possess one or multiple CBE sgRNA sequences. In addition to testing this in *L.*
358 *mexicana*, we also wanted to assess this for *L. donovani and L. major*, as we had not sequenced
359 respective mutants via ONT and Illumina sequencing.

360 Using again Cas12a crRNA-4 for the integration of a small-scale pTB105 CBE sgRNA expression
361 cassette library (containing 13 different CBE sgRNA sequences), we isolated 10 clones from each
362 species, PCR amplified the integrated CBE sgRNA locus, and sequenced it by Sanger sequencing.
363 As expected, we found only unique sequencing reads for all tested *L. mexicana* clones, confirming the
364 integration of only one guide per transfectant (Figure 4 S2). However, for *L. donovani* and *L. major*, 2
365 out of 10 sequencing reads showed mixed guide sequences (Figure 4 S2), suggesting that multiple
366 CBE sgRNAs can be integrated per cell, though at a slightly lower rate of about 20% compared to the
367 previous 38% observed with plasmid transfections. Furthermore, the integration of multiple sgRNAs
368 per cell remained random. While testing other Cas12a crRNAs in the future may identify a more
369 unique integration locus for *L. donovani* and *L. major* parasites, any compensatory effects through the
370 integration of multiple CBE sgRNAs in these species will likely be minimal and presumably not
371 detectable in large-scale screens with a high library representation rate. Therefore, we believe that
372 this method is suitable not only for screens in *L. mexicana* but also in *L. donovani* and *L. major*.

373 **Improved CBE sgRNA design to prioritize edits resulting only in STOP codons**

374 The results above demonstrate that Cas12a crRNAs can be used to efficiently integrate CBE sgRNA
375 expression cassettes into *L. mexicana*, *L. major* and *L. donovani*. This has no significant impact on
376 parasite growth and enables high editing rates in all these tested species. However, as we noted in
377 our previous study (Engstler and Beneke, 2023), high editing rates do not necessarily lead to a strong
378 knockdown of the targeted protein. Cells with a deleterious mutation can be simply outcompeted by
379 cells with a non-deleterious mutation. This issue is particularly relevant when not all available cytosine
380 nucleotides within the CBE sgRNA editing window result in a STOP codon after thymine conversion.
381 To address this, we have therefore improved the scoring of previously designed CBE sgRNAs by
382 implementing a C-score that determines the ratio of available cytosines to resulting STOP codons
383 (Figure 4 S3). This new scoring system has been uploaded to www.leishbaseedit.net. We also
384 considered the position at which the STOP codon would occur and designed a scoring matrix that
385 rates CBE sgRNAs higher when the STOP codon is introduced within positions 4-8 and lower when
386 introduced within positions 11-12 (Figure 4 S3). While our ratio scoring aims to increase the chance of
387 successfully generating a functional mutation through STOP codon insertion, it is important to note
388 that the introduction of a STOP codon is not the only efficient way to generate a functional mutant. As
389 shown above, the introduction of a thymidine homo-polymer ("TTTTT") within the PF16 CDS produces
390 the same motility phenotype observed when using gene replacement strategies for knockout

391 generation (Beneke et al., 2017). Ultimately, this expands the possibilities for upcoming mutational
392 screens in *Leishmania*.

393 **Co-expression of Cas12a and CBE enables a wide range of genetic manipulations**

394 While these modifications to our sgRNA scoring tool represent another improvement in our method,
395 the design of our triple expression construct (AsCas12a ultra, T7 RNAP, and Cas9 CBE) also offers
396 opportunities for other advancements. For example, it enables hybrid approaches where classical
397 CRISPR gene replacement and/or tagging methods can be combined with cytosine base editing
398 experiments in one cell line. This is particularly interesting for targeting multiple genes simultaneously
399 or dispersed multi-copy genes, and can also include the co-targeting of non-coding and coding
400 genetic elements. Furthermore, since Cas12a has an intrinsic RNA cleavage activity, multiplexing of
401 sgRNAs is possible and this expands the range of potential applications further.

402 To explore the applicability of AsCas12a ultra for gene replacement strategies, such as the
403 LeishGEdit approach (Beneke and Gluenz, 2019; Beneke and Gluenz, 2020; Beneke et al., 2017), we
404 devised two Cas12a crRNAs targeting the 5' and 3' UTR of the PF16 ORF (Figure 5A). Additionally,
405 we designed 30nt homology flanks adjacent to these crRNAs. We then PCR-amplified pTBlast and
406 pTPuro cassettes from the LeishGEdit toolbox using primers containing these homology flanks and
407 co-transfected them with Cas12a crRNA template DNA into *L. mexicana* parasites. These cells
408 contained the pTB107 construct for co-expression of AsCas12a ultra, T7 RNAP, and CBE. Like the
409 Cas9 LeishGEdit approach, transfected Cas12a crRNAs contained a T7 RNAP promoter for efficient
410 *in vivo* transcription (Figure 2B). Following transfection, we then confirmed that the ORF was
411 successfully replaced by drug resistance markers on both alleles and amplified the PF16 locus with
412 two ORF spanning primers (Figure 5A and B). In addition, we performed Sanger sequencing over
413 integration flanks to verify the integration of donor DNA fragments. This analysis confirmed the
414 accurate integration of both donor DNA constructs (Figure 5C and D). Lastly, we performed again our
415 motility analysis on these mutants, revealing the expected PF16 motility phenotype (Figure 5E).
416 Overall, this demonstrates the versatility of our AsCas12a ultra, T7 RNAP, and CBE co-expression
417 vector for a wide range of CRISPR applications in *Leishmania*.

418 **Conclusion**

419 The *Leishmania* research community faces significant challenges in targeting all genes within the
420 species. The absence of a functional NHEJ pathway complicates the process of obtaining null
421 mutants, typically demanding the additional use of donor DNA, selection of edits associated with drug
422 resistance, or the time-consuming isolation of clones. These complexities also apply to loss-of-
423 function screens. Classical pooled CRISPR transfection screening formats are unlikely to be executed
424 successfully, unless additional selective measures are used. While, bar-seq screens (Baker et al.,
425 2021; Beneke et al., 2019; Beneke and Gluenz, 2020) and RNAi methods (de Paiva et al., 2015; Lye
426 et al., 2022) offer potential solutions, they come with clear limitations. Most notably, the use of RNAi is
427 restricted to *Leishmania* species within the *Viannia* subgenus, and bar-seq screens pose logistical
428 challenges due to the necessity of generating thousands of individually created mutants. Furthermore,
429 CRISPR gene replacement approaches, such as bar-seq methods, require multiple rounds of

transfection when targeting dispersed multi-copy genes and are not suited to mutate interrupted tandemly arrayed coding and non-coding genes, which are abundantly present in the *Leishmania* genome.

Therefore, we recently introduced cytosine base editing as an alternative method for gene editing and large-scale screening in *Leishmania*, aiming to overcome these limitations. However, variations in editing efficiency, substantial reduction in parasite growth, competition between deleterious and non-deleterious mutations, and low transfection rates prompted further refinements of our method. Here we present major improvements that collectively enhance our CBE method for *Leishmania* parasites.

In our final setup, we effectively employ a dual construct system, where a stable cell line is transfected with a CBE sgRNA expression construct. The stable cell line expresses the hyBE4max CBE, AsCas12a ultra, and T7 RNAP, with CBE sgRNA expression driven by a T7 RNAP promoter variant (T7 T-10 GG). Alongside our updated CBE sgRNA design tool, which now prioritizes sgRNAs with a low cytosine to resulting STOP codon ratio, this system achieves high editing rates without affecting parasite growth. Compared to our initial CBE single-vector method, this dual-construct system has the disadvantage that it requires the generation of a stable cell line first. However, it offers the clear advantage that CBE sgRNA expression constructs can be efficiently integrated using AsCas12a-mediated DSBs. Through testing a series of Cas12a crRNAs, we identified a specific Cas12a crRNA capable of efficiently integrating CBE sgRNA expression cassettes into the 18S rRNA SSU safe harbor locus. CBE sgRNA expression cassettes can thereby be generated by amplification or digestion of the plasmid pTB105. In combination with the Lonza Nucleofector Technology, this approach increases transfection rates by ~400-fold, yielding up to 1 transfectant per 70 transfected cells. Additionally, the co-expression of Cas12a and CBE provides strategic advantages, enabling the use of CRISPR gene replacement and base editing approaches in the same cell line. Moreover, Cas12a can be easily employed for protein tagging and multiplexing of sgRNAs, offering in the future a wide range of possible editing experiments in combination with base editing. Overall, we believe that our improved toolbox sets the stage for various gene editing applications in *Leishmania*, including genome-wide cytosine base editor screens, and we hope that these will make significant advancements in the field.

459 **MATERIAL AND METHODS**

Key Resources Table				
Reagent type (species) or resource	**Designation**	**Source or reference**	**Identifiers**	**Additional information**
Cell line (*Leishmania mexicana*)	*L. mexicana* wildtype	Eva Gluenz laboratory	WHO strain MNYC/BZ/62/M379	Used TriTrypDB (release 59, (Aslett et al., 2010)) reference annotation: *L. mexicana* MHOMGT2001U1103
Cell line (*Leishmania major*)	*L. major* wildtype	Eva Gluenz laboratory	strain Friedlin	Used TriTrypDB (release 59, (Aslett et al., 2010)) reference annotation: *L. major* Friedlin
Cell line (*Leishmania donovani*)	*L. donovani* wildtype	Joachim Clos laboratory (Decuypere et al., 2005)	strain BPK190	Used TriTrypDB (release 59, (Aslett et al., 2010)) reference annotation: *L. donovani* BPK282A1
Recombinant DNA reagent	pTB007-hyBE4max	(Engstler and Beneke, 2023)		Contains CBE hyBE4max and T7 RNAP
Recombinant DNA reagent	pLdCH-hyBE4max	(Engstler and Beneke, 2023)		Contains CBE hyBE4max and CBE sgRNA
Recombinant DNA reagent	pLdCH-hyBE4max-LmajDBD	(Engstler and Beneke, 2023)		Contains Leishmania-optimised CBE hyBE4max and CBE sgRNA
Recombinant DNA reagent	pTB107	This study		Contains CBE hyBE4max, AsCas12a ultra and T7 RNAP
Recombinant DNA reagent	pTB106	This study		Contains Leishmania-optimised CBE hyBE4max, AsCas12a ultra and T7 RNAP
Recombinant DNA reagent	pTB102	This study		Contains T7 RNAP promoter-driven CBE sgRNA expression cassette without homology flanks
Recombinant DNA reagent	pTB104	This study		Contains T7 RNAP promoter-driven CBE sgRNA expression cassette with homology flanks for neomycin-resistance gene

Recombinant DNA reagent	pTB105	This study		Contains T7 RNAP promoter-driven CBE sgRNA expression cassette with homology flanks for 18S rRNA SSU locus
Software	TriTrypDB (release 59)	(Aslett et al., 2010)	https://tritrypdb.org/tritrypdb/app	
Software	LeishBASEedit	This study	http://www.leishbaseedit.net/	See description under "Automated CBE guide design using LeishBASEedit"
Gene (*L. donovani* BPK282A1, *L. major* Friedlin, *L. mexicana* MHOMGT2001U1103)	PF16	TriTrypDB (release 59) (Aslett et al., 2010)	LdBPK_201450.1, LmjF.20.1400, LmxM.20.1400	

460

461 **Cell culture**

462 As described in Engstler and Beneke (2023), promastigote-form *L. mexicana* (WHO strain
463 MNYC/BZ/62/M379), *L. major* Friedlin and *L. donovani* (strain BPK190, (Decuypere et al., 2005))
464 were grown at 28°C in M199 medium (Life Technologies) supplemented with 2.2 g/L NaHCO3,
465 0.0025% haemin, 0.1 mM adenine hemisulfate, 1.2 µg/mL 6-biopterin, 40 mM 4-(2-
466 Hydroxyethyl)piperazine-1-ethanesulfonic acid (HEPES) pH 7.4 and 20% FCS. Media were
467 supplemented with the relevant selection drugs: 40 µg/ml Hygromycin B, 40 µg/ml Puromycin
468 Dihydrochloride and 40 µg/ml G-418 Disulfate. The identity of each *Leishmania* species and absence
469 of mycoplasma contamination was confirmed previously (Engstler and Beneke, 2023). Doubling times
470 were determined as described in Engstler and Beneke (2023).

471 **Cas12a and CBE sgRNA design**

472 For optimizing the CBE targeting of tdTomato and PF16, we selected sgRNAs from Engstler and
473 Beneke (2023) (Supplementary File 1).

474 Cas12a crRNAs were designed using CCTop (Labuhn et al., 2018; Stemmer et al., 2015) with the
475 "PAM type" setting "TTTN" and species specification "Protists – Euglenozoa – *Leishmania tarentolae*".
476 For the Cas12a crRNA sequence search, we selected the 18S rRNA locus from *L. mexicana* (using
477 an ONT-Illumina sequencing optimised MHOMGT2001U1103 genome annotation from Beneke et al.
478 (2022)) and selected homology flanks routinely used for integration into this locus (Misslitz et al., 2000;
479 Sorensen et al., 2003). For designing Cas12a crRNAs that would target a potential "landing-pad", we
480 searched the neomycin-resistance marker for possible spacer sequences. All resulting Cas12a
481 crRNAs were then checked for possible off-targets by using a local blast search against all
482 *Leishmania* species currently available on TritrypDB (release 59, (Aslett et al., 2010)). This ensures
483 that Cas12a crRNAs can be used for specific donor DNA integration in these species.

484 **Plasmid construction**

485 All generated plasmids were subjected to whole plasmid sequencing at Plasmidsaurus and critical
486 sites, were additionally subjected to Sanger sequencing.

487 Primers were all ordered as standard desalted oligos at 25 nmole scale (Sigma). All oligo sequences
488 can be found in Supplementary File 1. Plasmid maps are contained within Supplementary File 2 and
489 can also be downloaded from www.leishbaseedit.net.

490 **Construction of CBE, Cas12a and T7 RNAP co-expression plasmids**

491 We synthesized the open-reading frame (ORF) of AsCas12a ultra (M537R/F870L mutation) (Zhang et
492 al., 2021) with a fused SV40 nuclear localisation signal (NLS), a 3xFLAG tag, a P2A self-cleaving
493 peptide and a c-myc NLS, consisting of six repeats. This c-myc NLS repeat has been previously
494 shown to increase editing activity (Gier et al., 2020). We then amplified the synthesized Cas12a
495 construct in a fusion PCR, adding parts of the T7 RNAP (ORF) and an intergenic region to the

496 construct (using primer-pair 2051F/2052R and 2053F/2054R for amplification from pTB007-
497 hyBE4max). Subsequently, this enabled cloning of the AsCas12a-expression cassette into pTB007-
498 hyBE4max using FseI and AflII. We termed the resulting plasmid pTB107, which allows for the co-
499 expression of AsCas12a ultra, T7 RNAP, hyBE4max CBE and hygromycin resistance-marker. To
500 create a version of pTB107 that contained our previously pioneered *Leishmania*-derived version of the
501 Rad51 single-stranded DNA-binding domain (ssDNA-DBD), we digested pLdCH-hyBE4max-LmajDBD
502 (Engstler and Beneke, 2023) and pTB107 with AvrII and FseI to generate pTB106.

503 **Construction of sgRNA expression plasmids and their optimisation by promoter testing**

504 For generation of T7 RNAP promoter-driven CBE sgRNA expression plasmids, we amplified and
505 cloned the sgRNA-expression cassette from pLdCH into NsiI and MluI sites of a pPLOT-Puro plasmid
506 (Beneke et al., 2017), thereby introducing the unmodified T7 RNAP promoter sequence (amplification
507 using primer-pair 2128F-WT/2129R). To enable sgRNA cloning using BbsI sites, we then eliminated
508 the BbsI site contained within the Actin 5'UTR of this plasmid, using primer-pair 2126F/2129R and
509 PspOMI/MluI restriction sites. To avoid over-expression of the puromycin drug resistance marker, we
510 also eliminated the additional unmodified T7 RNAP promoter sequence contained in the plasmid
511 backbone by amplifying the whole expression cassette (using primer-pair 2067F/2068R) and cloning it
512 using PacI into the bacterial backbone of plasmid pTB007 (Beneke et al., 2017). We then cloned into
513 this resulting plasmid T7 RNAP and rRNAP promoter variant cassettes, containing tdTomato targeting
514 sgRNAs, by using again NsiI and MluI sites (primer-pairs 2014-2021 and 2025-2027). Tdtomato-
515 targeting sgRNA expression constructs were then transfected as episomes into *L. major* parasites
516 that expressed a tdTomato reporter, T7 RNAP and CBE. Following transfection recovery, the
517 proportion of tdTomato-expressing cells was determined by FACS analysis and doubling times
518 measured. Thereby, transfection and FACS analysis were carried out as described previously
519 (Engstler and Beneke, 2023). Following promoter testing, we then finalized our design and generated
520 pTB102 with a T7 RNAP T10 GG promoter variant (using primer-pair 2128F-T10GG/2129R).

521 To include homology flanks in the pTB102 plasmid, neomycin-targeting or 18S rRNA-targeting
522 regions were amplified and fused to pTB102 sgRNA expression cassettes using a fusion PCR
523 approach (primer-pairs 2236F-2257R). Resulting amplicons were cloned into PacI sites, resulting in
524 pTB104 (neomycin-targeting T7 RNAP expression plasmid) and pTB105 (18S rRNA-targeting T7
525 RNAP expression plasmid).

526 PF16 and tdTomato targeting CBE sgRNAs were cloned into pTB102, pTB104 and pTB105 plasmids
527 using BbsI sites as previously described (Engstler and Beneke, 2023).

528 **Preparation of donor DNA and Cas12a crRNA template DNA**

529 To amplify the CBE sgRNA expression donor construct, 50 ng of plasmid template (pTB102, pTB104
530 or pTB105) containing a CBE targeting guide, 200 µM dNTPs, 0.5 µM each of forward and reverse
531 primers, and 1 unit of Q5 polymerase (New England Biolabs) were mixed in 1x Q5 buffer to a final
532 volume of 100 µl. Oligos used for amplification contained homology flanks of varying lengths. PCR

533 steps were 30 s at 98°C, followed by 20 cycles of 10 s at 98°C, 10 s at 65°C and 40 s at 72°C,
534 concluding with a final elongation step of 5 min at 72°C. Alternatively, donor DNA was produced by
535 digesting pTB104 and pTB105 plasmids with PacI. To confirm the presence of the expected product,
536 2 µl of this reaction was analysed on a 0.8% agarose gel.

537 For the amplification of the Cas12a crRNA template DNA, we used a common forward primer,
538 containing an unmodified T7 RNAP promoter sequence and an optimised Cas12a direct repeat (DR)
539 from DeWeirdt et al. (2021). For the PCR 200 µM dNTPs, 2 µM each of Cas12a forward primer and
540 corresponding reverse primer, and 1 unit of Phusion Polymerase (Thermo Fisher) were mixed in 1x
541 Phusion GC Buffer and 3 % DMSO to a total volume of 50 µl. PCR steps were 30 s at 98°C followed
542 by 35 cycles of 10 s at 98°C, 10 s at 65°C and 10s at 72° concluding with a final elongation step for 7
543 min at 72°C. Successful amplification was confirmed by running 2 µl of the reaction on a 2% agarose
544 gel.

545 The remainder of the donor and crRNA reaction was combined, EtOH purified, resuspended in 50 µl
546 ultra-pure water, heat sterilised at 95°C for 5 min and then used for transfection.

547 **Testing Cas12a-mediated integration of mNG constructs**

548 To test the Cas12a-mediated integration efficiency of donor DNA constructs with varying homology
549 flank lengths, we generated a DNA construct containing mNeonGreen (mNG) as a reporter and
550 blasticidin as a resistance marker, as well as ~600 nt homology flanks targeting the 18S rRNA SSU
551 locus (Misslitz et al., 2000; Sorensen et al., 2003). This construct was assembled by fusion PCR as
552 previously described (Engstler and Beneke, 2023), using pPLOT-mNG-Blast (Beneke et al., 2017) as
553 a PCR template. The generated fusion construct was then cloned into a blunted vector backbone,
554 resulting in the plasmid pPLOT-SSU-HDR-mNG-Blast.

555 We then PCR amplified as described above donor DNA from this plasmid with varying homology flank
556 lengths (~600 nt, 60 nt and 30 nt; Supplementary File 1). Resulting PCR amplicons and the pPLOT-
557 SSU-HDR-mNG-Blast plasmid itself were then purified using ethanol precipitation and normalized to
558 the same number of DNA molecules (3.6×10^{12} molecules per transfection). This normalization was
559 based on 10 µg of pPLOT-SSU-HDR-mNG-Blast plasmid. In addition, 10 µg of Cas12a crRNA
560 template DNA was added to donor DNA as indicated (Figure 2). As described previously (Engstler
561 and Beneke, 2023), DNA mixtures were then transfected using 5×10^{6} cells per transfection and we
562 determined the number of blasticidin resistant clones by immediately diluting transfected populations
563 and platting them on 96 well plates. In addition, 10 days post transfection undiluted blasticidin
564 resistant populations were subjected to FACS analysis. To verify the correct integration of donor DNA,
565 DNA was isolated from these populations as described (Engstler and Beneke, 2023; Rotureau et al.,
566 2005) and amplified integration sites were submitted for Sanger sequencing at Eurofins Genomics
567 (Figure 2 S1A and D).

568

569 **High efficiency transfections**

570 Transfections were generally carried out as described in Engstler and Beneke (2023), transfecting
571 ~5×10^6 cells in 1x Tb-BSF buffer (Schumann Burkard et al., 2011) using 2 mm cuvettes (BTX) with an
572 Amaxa Nucleofector 2b (Lonza, program X-001).

573 For high efficiency transfections, we modified the protocol and compared site-by-site the transfection
574 efficiency of the Basic Parasite Nucleofector Kit (Lonza) and Tb-BSF protocol (Schumann Burkard et
575 al., 2011). 1×10^8 or 2.5×10^8 cells were collected, washed once in 1x Tb-BSF buffer and resuspended
576 in either 100 µl Lonza transfection reagent or 200 µl Tb-BSF buffer. 10 µg donor DNA and 10 µg
577 Cas12a crRNA template DNA were diluted in either 20 µl (Lonza transfection) or 50 µl (Tb-BSF
578 transfection) ultrapure water, heat sterilized and added to each transfection respectively (final
579 transfection volume Tb-BSF 250 µl, Lonza 120 µl). Cells were transfected using transfection cuvettes
580 supplied with the Basic Parasite Nucleofector Kit (Lonza transfection) or 2 mm BTX cuvettes (Tb-BSF
581 transfection) with one pulse of the X-001 program on an Amaxa Nucleofector 2b (Lonza). For
582 measuring transfection efficiencies, cells were selected and diluted on 96-well plates as described
583 (Engstler and Beneke, 2023).

584 **Targeting of PF16 with an improved CBE system**

585 For testing the editing efficiency of our improved CBE system, we amplified donor DNA from the
586 pTB102 plasmid, containing the sgRNA PF16-3 from Engstler and Beneke (2023). As indicated
587 (Figure 4), donor DNAs were mixed with respective Cas12a crRNA DNA templates and transfected
588 into *Leishmania* parasites. Following selection and the recovery of parasites, mutants were tracked in
589 duplicates or triplicates and their mean velocity determined as described before (Engstler and Beneke,
590 2023). Editing rates were measured by amplifying the PF16 target locus and by subjecting PCR
591 amplicons to Sanger sequencing (Engstler and Beneke, 2023).

592 **ONT and Illumina sequencing analysis of CBE PF16 mutants**

593 DNA from *L. mexicana* CBE PF16 mutants was isolated as previously described (Engstler and
594 Beneke, 2023; Rotureau et al., 2005) and submitted for ONT and Illumina sequencing at
595 Plasmidsaurus (service: “Big Hybrid ONT + Illumina”). Obtained raw fastq files from ONT and Illumina
596 sequencing were then assembled using the Burrows-Wheeler Aligner (Li and Durbin, 2009) using two
597 customized *L. mexicana* genomes of the MHOMGT2001U1103 annotation. In the first genome, we
598 duplicated chromosome 27 and modified the 18S rRNA SSU locus of one chromosome 27 copy to
599 include the tdTomato expression cassette (Engstler and Beneke, 2023) (Figure 4 S1B), while the
600 other copy contained the CBE sgRNA expression construct. In the second genome, we instead
601 modified chromosome 27 to contain both expression cassettes consecutively (Figure 4 S1C).
602 Following alignments, we then used samtools (Li et al., 2009) for sorting and indexing of bam files and
603 viewed our analysis using the IGV genome browser (Robinson et al., 2011).

604 **Optimised CBE sgRNA scoring**

605 To determine the likelihood of successful gene editing, we adjusted the sgRNA ranking system. New
606 sgRNA ranking scores were calculated based on various parameters, including the relative likelihood
607 of generating a STOP codon from a cytosine base, the total number of possible STOP codons, the
608 location of cytosines within the editing window, and the position of the guide's target within the coding
609 sequence (CDS) of the gene. To generate the overall score, we weighted the contribution of each of
610 these scores, with the likelihood of generating a stop codon having four times more contribution than
611 the other scores. We then normalized the total score on a scale of 0 to 100, where 0 represents the
612 best score, and 100 represents the worst score.

613 The updated data sets and code can be accessed at http://www.leishbaseedit.net/ and
614 https://github.com/ElisabethMeiser/Collaboration_Beneke_Meiser, respectively.

615 **Cas12a-mediated gene replacement for generation of knockout cell lines**

616 For the Cas12a-mediated replacement of the PF16 CDS, we adapted the LeishGEdit approach
617 (Beneke and Gluenz, 2019; Beneke and Gluenz, 2020; Beneke et al., 2017) and PCR-amplified two
618 Cas12a crRNAs targeting the 5' and 3' UTR of the PF16 ORF (crRNA design as described above). In
619 addition, we PCR-amplified pTBlast and pTPuro cassettes from the LeishGEdit toolbox with primers
620 containing 30 nt homology flanks adjacent to these crRNAs. Both PCRs were carried out as described
621 above and we then co-transfected all resulting products into *L. mexicana* cells containing the pTB107
622 plasmid. Successful gene replacement was confirmed by amplifying and Sanger sequencing the
623 PF16 locus with two ORF spanning primers.

624

AVAILABILITY

All data generated or analysed during this study are included in the manuscript and supplementary file. LeishBASEedit is an open-source primer design tool available under www.leishbaseedit.net.

ACKNOWLEDGEMENT

We thank all members of the Alsheimer, Engstler, Janzen and Kramer group for helpful discussions and support. In addition, we thank Markus Engstler for providing research resources and helpful comments on the manuscript. This project was funded by Tom Beneke through an EMBO Postdoctoral Fellowship (ALTF 727-2021) and Marie Skłodowska-Curie Actions Postdoctoral Fellowship (101064428 – LeishMOM).

CONFLICT OF INTEREST

All authors declare that they have no conflicts of interest.

636 **REFERENCES**

637 **Aslett, M., Aurrecoechea, C., Berriman, M., Brestelli, J., Brunk, B. P., Carrington, M.,**
638 **Depledge, D. P., Fischer, S., Gajria, B., Gao, X. et al.** (2010). TriTrypDB: a functional genomic
639 resource for the Trypanosomatidae. *Nucleic Acids Res* **38**, D457-62.
640 **Baker, N., Catta-Preta, C. M. C., Neish, R., Sadlova, J., Powell, B., Alves-Ferreira, E. V. C.,**
641 **Geoghegan, V., Carnielli, J. B. T., Newling, K., Hughes, C. et al.** (2021). Systematic functional analysis
642 of Leishmania protein kinases identifies regulators of differentiation or survival. *Nat Commun* **12**,
643 1244.
644 **Beneke, T., Demay, F., Hookway, E., Ashman, N., Jeffery, H., Smith, J., Valli, J., Becvar, T.,**
645 **Myskova, J., Lestinova, T. et al.** (2019). Genetic dissection of a Leishmania flagellar proteome
646 demonstrates requirement for directional motility in sand fly infections. *PLoS Pathog* **15**, e1007828.
647 **Beneke, T., Dobramysl, U., Catta-Preta, C. M. C., Mottram, J. C., Gluenz, E. and Wheeler, R.**
648 **J.** (2022). Genome sequence of Leishmania mexicana MNYC/BZ/62/M379 expressing Cas9 and T7
649 RNA polymerase. *Wellcome Open Res* **7**, 294.
650 **Beneke, T. and Gluenz, E.** (2019). LeishGEdit: A Method for Rapid Gene Knockout and
651 Tagging Using CRISPR-Cas9. *Methods Mol Biol* **1971**, 189-210.
652 **Beneke, T. and Gluenz, E.** (2020). Bar-seq strategies for the LeishGEdit toolbox. *Mol Biochem*
653 *Parasitol* **239**, 111295.
654 **Beneke, T., Madden, R., Makin, L., Valli, J., Sunter, J. and Gluenz, E.** (2017). A CRISPR Cas9
655 high-throughput genome editing toolkit for kinetoplastids. *R Soc Open Sci* **4**, 170095.
656 **Burge, R. J., Damianou, A., Wilkinson, A. J., Rodenko, B. and Mottram, J. C.** (2020).
657 Leishmania differentiation requires ubiquitin conjugation mediated by a UBC2-UEV1 E2 complex.
658 *PLoS Pathog* **16**, e1008784.
659 **Burkard, G., Fragoso, C. M. and Roditi, I.** (2007). Highly efficient stable transformation of
660 bloodstream forms of Trypanosoma brucei. *Mol Biochem Parasitol* **153**, 220-3.
661 **Damianou, A., Burge, R. J., Catta-Preta, C. M. C., Geoghegan, V., Nievas, Y. R., Newling, K.,**
662 **Brown, E., Burchmore, R., Rodenko, B. and Mottram, J. C.** (2020). Essential roles for
663 deubiquitination in Leishmania life cycle progression. *PLoS Pathog* **16**, e1008455.
664 **de Paiva, R. M., Grazielle-Silva, V., Cardoso, M. S., Nakagaki, B. N., Mendonca-Neto, R. P.,**
665 **Canavaci, A. M., Souza Melo, N., Martinelli, P. M., Fernandes, A. P., daRocha, W. D. et al.** (2015).
666 Amastin Knockdown in Leishmania braziliensis Affects Parasite-Macrophage Interaction and Results
667 in Impaired Viability of Intracellular Amastigotes. *PLoS Pathog* **11**, e1005296.
668 **Decuypere, S., Rijal, S., Yardley, V., De Doncker, S., Laurent, T., Khanal, B., Chappuis, F. and**
669 **Dujardin, J. C.** (2005). Gene expression analysis of the mechanism of natural Sb(V) resistance in
670 Leishmania donovani isolates from Nepal. *Antimicrob Agents Chemother* **49**, 4616-21.
671 **DeWeirdt, P. C., Sanson, K. R., Sangree, A. K., Hegde, M., Hanna, R. E., Feeley, M. N.,**
672 **Griffith, A. L., Teng, T., Borys, S. M., Strand, C. et al.** (2021). Optimization of AsCas12a for
673 combinatorial genetic screens in human cells. *Nat Biotechnol* **39**, 94-104.
674 **Engstler, M. and Beneke, T.** (2023). Gene editing and scalable functional genomic screening
675 in Leishmania species using the CRISPR/Cas9 cytosine base editor toolbox LeishBASEedit. *Elife* **12**.
676 **Gier, R. A., Budinich, K. A., Evitt, N. H., Cao, Z., Freilich, E. S., Chen, Q., Qi, J., Lan, Y., Kohli,**
677 **R. M. and Shi, J.** (2020). High-performance CRISPR-Cas12a genome editing for combinatorial genetic
678 screening. *Nat Commun* **11**, 3455.
679 **Glover, L., Alsford, S., Baker, N., Turner, D. J., Sanchez-Flores, A., Hutchinson, S., Hertz-**
680 **Fowler, C., Berriman, M. and Horn, D.** (2015). Genome-scale RNAi screens for high-throughput
681 phenotyping in bloodstream-form African trypanosomes. *Nat Protoc* **10**, 106-33.
682 **Glover, L. and Horn, D.** (2009). Site-specific DNA double-strand breaks greatly increase
683 stable transformation efficiency in Trypanosoma brucei. *Mol Biochem Parasitol* **166**, 194-7.
684 **Horn, D.** (2022). Genome-scale RNAi screens in African trypanosomes. *Trends Parasitol* **38**,
685 160-173.

686 **Labuhn, M., Adams, F. F., Ng, M., Knoess, S., Schambach, A., Charpentier, E. M., Schwarzer,**
687 **A., Mateo, J. L., Klusmann, J. H. and Heckl, D.** (2018). Refined sgRNA efficacy prediction improves
688 large- and small-scale CRISPR-Cas9 applications. *Nucleic Acids Res* **46**, 1375-1385.
689 **Li, H. and Durbin, R.** (2009). Fast and accurate short read alignment with Burrows-Wheeler
690 transform. *Bioinformatics* **25**, 1754-60.
691 **Li, H., Handsaker, B., Wysoker, A., Fennell, T., Ruan, J., Homer, N., Marth, G., Abecasis, G.,**
692 **Durbin, R. and Genome Project Data Processing, S.** (2009). The Sequence Alignment/Map format
693 and SAMtools. *Bioinformatics* **25**, 2078-9.
694 **Lye, L. F., Owens, K., Shi, H., Murta, S. M., Vieira, A. C., Turco, S. J., Tschudi, C., Ullu, E. and**
695 **Beverley, S. M.** (2010). Retention and loss of RNA interference pathways in trypanosomatid
696 protozoans. *PLoS Pathog* **6**, e1001161.
697 **Lye, L. F., Owens, K. L., Jang, S., Marcus, J. E., Brettmann, E. A. and Beverley, S. M.** (2022).
698 An RNA Interference (RNAi) Toolkit and Its Utility for Functional Genetic Analysis of Leishmania
699 (Viannia). *Genes (Basel)* **14**.
700 **Martel, D., Beneke, T., Gluenz, E., Spath, G. F. and Rachidi, N.** (2017). Characterisation of
701 Casein Kinase 1.1 in Leishmania donovani Using the CRISPR Cas9 Toolkit. *Biomed Res Int* **2017**,
702 4635605.
703 **Misslitz, A., Mottram, J. C., Overath, P. and Aebischer, T.** (2000). Targeted integration into a
704 rRNA locus results in uniform and high level expression of transgenes in Leishmania amastigotes.
705 *Mol Biochem Parasitol* **107**, 251-61.
706 **Morris, J. C., Wang, Z., Drew, M. E. and Englund, P. T.** (2002). Glycolysis modulates
707 trypanosome glycoprotein expression as revealed by an RNAi library. *EMBO J* **21**, 4429-38.
708 **Padmanabhan, R., Sarcar, S. N. and Miller, D. L.** (2020). Promoter Length Affects the
709 Initiation of T7 RNA Polymerase In Vitro: New Insights into Promoter/Polymerase Co-evolution. *J Mol*
710 *Evol* **88**, 179-193.
711 **Passos-Silva, D. G., Rajao, M. A., Nascimento de Aguiar, P. H., Vieira-da-Rocha, J. P.,**
712 **Machado, C. R. and Furtado, C.** (2010). Overview of DNA Repair in Trypanosoma cruzi, Trypanosoma
713 brucei, and Leishmania major. *J Nucleic Acids* **2010**, 840768.
714 **Paul, B. and Montoya, G.** (2020). CRISPR-Cas12a: Functional overview and applications.
715 *Biomed J* **43**, 8-17.
716 **Robinson, J. T., Thorvaldsdottir, H., Winckler, W., Guttman, M., Lander, E. S., Getz, G. and**
717 **Mesirov, J. P.** (2011). Integrative genomics viewer. *Nat Biotechnol* **29**, 24-6.
718 **Rotureau, B., Gego, A. and Carme, B.** (2005). Trypanosomatid protozoa: a simplified DNA
719 isolation procedure. *Exp Parasitol* **111**, 207-9.
720 **Sanjana, N. E., Shalem, O. and Zhang, F.** (2014). Improved vectors and genome-wide
721 libraries for CRISPR screening. *Nat Methods* **11**, 783-784.
722 **Schumann Burkard, G., Jutzi, P. and Roditi, I.** (2011). Genome-wide RNAi screens in
723 bloodstream form trypanosomes identify drug transporters. *Mol Biochem Parasitol* **175**, 91-4.
724 **Schumann, G., Kangussu-Marcolino, M. M., Doiron, N., Kaser, S., de Assis Burle-Caldas, G.,**
725 **DaRocha, W. D., Teixeira, S. M. and Roditi, I.** (2017). Zinc finger nuclease technology: A stable tool
726 for high efficiency transformation in bloodstream form T. brucei. *Mol Biochem Parasitol* **213**, 12-15.
727 **Sorensen, M., Lippuner, C., Kaiser, T., Misslitz, A., Aebischer, T. and Bumann, D.** (2003).
728 Rapidly maturing red fluorescent protein variants with strongly enhanced brightness in bacteria.
729 *FEBS Lett* **552**, 110-4.
730 **Stemmer, M., Thumberger, T., Del Sol Keyer, M., Wittbrodt, J. and Mateo, J. L.** (2015).
731 CCTop: An Intuitive, Flexible and Reliable CRISPR/Cas9 Target Prediction Tool. *PLoS One* **10**,
732 e0124633.
733 **Ullu, E., Tschudi, C. and Chakraborty, T.** (2004). RNA interference in protozoan parasites.
734 *Cell Microbiol* **6**, 509-19.
735 **Wirtz, E., Hoek, M. and Cross, G. A.** (1998). Regulated processive transcription of chromatin
736 by T7 RNA polymerase in Trypanosoma brucei. *Nucleic Acids Res* **26**, 4626-34.

Yau, E. H. and Rana, T. M. (2018). Next-Generation Sequencing of Genome-Wide CRISPR Screens. *Methods Mol Biol* **1712**, 203-216.

Zhang, L., Zuris, J. A., Viswanathan, R., Edelstein, J. N., Turk, R., Thommandru, B., Rube, H. T., Glenn, S. E., Collingwood, M. A., Bode, N. M. et al. (2021). AsCas12a ultra nuclease facilitates the rapid generation of therapeutic cell medicines. *Nat Commun* **12**, 3908.

Zhang, W. W., Lypaczewski, P. and Matlashewski, G. (2017). Optimized CRISPR-Cas9 Genome Editing for Leishmania and Its Use To Target a Multigene Family, Induce Chromosomal Translocation, and Study DNA Break Repair Mechanisms. *mSphere* **2**.

Zhang, W. W. and Matlashewski, G. (2015). CRISPR-Cas9-Mediated Genome Editing in Leishmania donovani. *MBio* **6**, e00861.

Zhang, W. W. and Matlashewski, G. (2019). Single-Strand Annealing Plays a Major Role in Double-Strand DNA Break Repair following CRISPR-Cas9 Cleavage in Leishmania. *mSphere* **4**.

Zhang, W. W., Wright, D. G., Harrison, L. and Matlashewski, G. (2022). Reconstitution of Mycobacterium marinum Nonhomologous DNA End Joining Pathway in Leishmania. *mSphere* **7**, e0015622.

Zhang, X., Chen, L., Zhu, B., Wang, L., Chen, C., Hong, M., Huang, Y., Li, H., Han, H., Cai, B. et al. (2020). Increasing the efficiency and targeting range of cytidine base editors through fusion of a single-stranded DNA-binding protein domain. *Nat Cell Biol* **22**, 740-750.

756 **FIGURE LEGENDS**

757 **Figure 1. Optimisation of CBE sgRNA expression in *L. major*.** Schematics of base editing
758 strategies to transfect *Leishmania* parasites either with a (**A**) single or (**B**) dual base editing system.
759 (**A**) Plasmid pLdCH-hyBE4max (Engstler and Beneke, 2023) contains (from left to right) a *L.*
760 *donovani*-derived ribosomal RNA (rRNA) promoter, single-guide RNA (sgRNA) expression cassette,
761 hepatitis delta virus (HDV) ribozyme containing transsplice sequence (TSS), hyBE4max CBE, *L.*
762 *donovani*-derived A2 intergenic sequence, and hygromycin resistance marker. (**B**) Plasmid pTB007-
763 hyBE4max (Engstler and Beneke, 2023) contains separated through intergenic regions (from left to
764 right) a hyBE4max CBE, T7 RNAP and hygromycin resistance marker. This construct is integrated
765 into the β-tubulin locus of *L. major* parasites (LmjF.33:339,096–341,104). The CBE sgRNA
766 expression vector contains a puromycin resistance marker, T7 RNAP promoter, single-guide RNA
767 (sgRNA) expression cassette and HDV ribozyme. (**C**) Different versions of the T7 RNAP promoter for
768 CBE sgRNA expression have been tested. (**D**) Doubling times of tdTomato-expressing *L. major*
769 parasites transfected with the single plasmid system and variants of the dual plasmid system for
770 targeting of tdTomato. Error bars show standard deviations of triplicates. Tar: Cells transfected with a
771 CBE sgRNA expression plasmid that facilitates the introduction of a STOP codon within the tdTomato
772 ORF; Ctrl: Cells transfected with a CBE sgRNA expression plasmid that causes a codon mutation
773 without amino acid change. Asterisks indicate Student's t-test: *p > 0.05. (**E**) FACS plot of parasites
774 shown in (**D**), analysed 7 days post transfection. (**F**) FACS plot showing tdTomato-expressing and
775 wildtype *L. major* parasites.

776 **Figure 2. Developing an AsCas12a-mediated integration system.** (**A**) Schematic of the Cas12a-
777 mediated integration approach. A stable *L. mexicana* cell line maintains plasmid pTB107 as an
778 episome and is co-transfected with a donor DNA reporter construct and a Cas12a crRNA template
779 DNA. Using a T7 RNAP promoter, the Cas12a crRNA template DNA is *in vivo* transcribed to facilitate
780 a Cas12a-mediated DSB at the 18S rRNA SSU locus. Using homology flanks the reporter construct is
781 efficiently integrated at the site of the DSB. Plasmid pTB107 thereby allows for the expression of
782 hyBE4max CBE, AsCas12a ultra (Zhang et al., 2021), T7 RNAP and hygromycin resistance marker.
783 AsCas12a ultra and T7 RNAP are expressed as a fusion protein but then cleaved through a P2A self-
784 cleaving peptide. The reporter constructs consists of a pPLOT plasmid tagging cassette (Beneke et
785 al., 2017) with additional homology flanks, allowing for the expression of mNeonGreen and a
786 blasticidin resistance marker. (**B**) Schematic of the Cas12a crRNA template DNA generation. Two
787 overlapping primers are amplified in a PCR reaction. The forward primer is common and contains an
788 unmodified T7 RNAP promoter and an optimised Cas12a direct repeat variant (DR) (DeWeirdt et al.,
789 2021). The guide reverse primer contains the crRNA specific spacer sequence aligning to the
790 targeted locus and the Cas12a DR to enable the overlap with the forward primer. (**C** and **E**) FACS plot
791 showing *L. mexicana* pTB107 parasites following the transfection described in (**A**). Percentages
792 represent the remaining proportion of mNeonGreen-expressing cells. (**C**) The homology flank (HF)
793 length used for reporter construct integration has been varied and the additional use of Cas12a
794 crRNA was tested. The transfection of a circular plasmid, containing the reporter construct was

795 included as a control (episomal). (**E**) Six different Cas12a crRNAs have been tested using two
796 different integration loci (as described in the main text). (**D** and **F**) Efficiency of transfections shown in
797 (**C** and **E**) were measured. The number of cells required for the transfection to obtain one transfectant
798 is shown. Error bars show standard deviations of triplicates.

799 **Figure 2 S1. Verification of AsCas12a-mediated reporter construct integration.** (**A**) Locus map of
800 the 18S rRNA SSU locus in *L. mexicana pTB107* cells before and after co-transfection of Cas12a
801 crRNA-1 and a reporter construct (as described in Figure 2A, C and D). The positions of Cas12a
802 crRNA-1 and HFs used for the integration of the reporter are highlighted. Amplicons of PCR reactions
803 spanning the integration sites are indicated and amplification results are shown in (**B**), with DNA sizes
804 highlighted in bp. (**C**) Sanger sequencing trace plots of amplicons shown in (**B**). The site of integration
805 into the 18S rRNA locus is highlighted with a dotted line. (**D**) Locus map of the 18S rRNA SSU locus
806 in *L. mexicana pTB107* cells expressing tdTomato before and after co-transfection of various Cas12a
807 crRNAs and a reporter construct (as described in Figure 2A, E and F). The positions of Cas12a
808 crRNA-1, 2, 3, 4, 5 and 6 are highlighted. Indicated HF positions have been used for the integration of
809 the tdTomato expression construct on one allele but individual HFs adjacent to crRNA-1 to 6 have
810 been used for integration of the reporter construct. Amplicons of PCR reactions spanning the
811 integration sites are indicated and amplification results are shown in (**E**) for verification of crRNA-4. (**F**)
812 Sanger sequencing trace plots of amplicons shown in (**E**).

813 **Figure 3. Integration of CBE sgRNA expression cassettes via AsCas12a ultra.** (**A**) Schematic of
814 Cas12a-mediated integration of the CBE sgRNA expression construct. The pTB107 stable cell line is
815 co-transfected with two constructs: (1) a Cas12a crRNA template DNA and (2) a CBE sgRNA
816 expression construct. The Cas12a crRNA template DNA is *in vivo* transcribed and consists of an
817 unmodified T7 RNAP promoter (T7wt, light green), a Cas12a direct repeat (DR, red) and a 20 nt
818 Cas12a guide target sequence (SPACER, blue). The CBE sgRNA expression construct is integrated
819 into the 18s rRNA SSU locus, following the Cas12a-mediated DSB. This donor construct contains two
820 homology flanks (HF, yellow), a puromycin-resistance marker (grey), a T7 T-10 GG promoter (green),
821 a guide target sequence (orange), a Cas9 scaffold (dark green) and an HDV (purple). (**B**) FACS plots
822 show pTB107 parasites that express tdTomato and have been transfected with pTB104 and pTB105
823 CBE sgRNA expression cassettes, containing a tdTomato-targeting guide. Percentages represent the
824 remaining proportion of tdTomato-expressing cells. (**C**) Following dilutions after transfection, the
825 number of puromycin-resistant transfectants obtained per transfected cell was calculated. Error bars
826 show standard deviations of triplicates. (**D**) Doubling times for transfected *Leishmania* parasites
827 shown in (**B**). PAR: parental cell line, UT: Un-transfected control.

828 **Figure 4. Targeting PF16 via Cas12a-delivered CBE sgRNA expression cassettes.** *L. major*, *L.*
829 *mexicana*, *L. donovani* wildtype and tdTomato/pTB107 cell lines were transfected with a range of CBE
830 sgRNA expression constructs in order to functionally mutate PF16. Different strategies for construct
831 delivery and sgRNA expression were tested, including the integration of constructs into the neomycin-
832 resistance marker (using Cas12a sgRNA-6) and the 18S rRNA SSU locus (Cas12a sgRNA-4), each
833 using 60 nt homology flanks. For comparison to our previous system (Engstler and Beneke, 2023), we

also expressed CBE sgRNAs from an episome and transfected pLdCH-hyBE4max into *L. major*. (**A**) Violin plot of pooled replicates from motility tracked non-clonal populations. The mean velocity of tracked cells was plotted 14 days post transfection for *L. major*, and 6 and 16 days post transfection for *L. mexicana* and *L. donovani*. The total percentage of tracked cells showing a velocity of less than 1 µm/s is highlighted. Each population was analysed using a Cramér-von Mises Test to detect any shift in the population distribution towards lower speed. Percentages are marked with an asterisks when that shift was significant (*p > 0.05). (**B**) Corresponding Sanger sequencing trace plots. Blue shading: 20 nt guide target sequence. Red dotted lines: hyBE4max editing window.

Figure 4 S1. ONT and Illumina sequencing of transfectants. *L. mexicana* pTB107 cells expressing tdTomato were co-transfected with Cas12a crRNA-4 template DNA constructs and a CBE sgRNA expression cassette containing a PF16 targeting guide sequence. Isolated DNA from parasites were subjected to ONT and Illumina sequencing 16 days post transfection. (**A**) Illumina sequencing reads were mapped against the *L. mexicana* MHOMGT2001U1103 genome annotation. The edited consensus sequence is shown alongside with the reference sequence and calculated editing rates (based on 35× genome coverage). (**B** and **C**) ONT reads were mapped against two customized *L. mexicana* MHOMGT2001U1103 genome annotations and viewed in the IGV genome browser (Robinson et al., 2011), with uniquely mapped reads in grey and reads with multiple alignments in white. Reads mapped against the PGKB 5' and 3'UTR are over-represented as these UTRs are also present in the pTB107 plasmid. (**B**) ONT reads were mapped to a customized genome in which we assumed that the 18S rRNA SSU locus had one integrated copy of the tdTomato expression cassette on one allele and one integrated copy of the CBE sgRNA expression construct on the other allele. Schematics show the annotation of genetic elements assumed to be on each allele. The position of one allele in respect to the position on the other allele is indicated with red arrows. The position of the Cas12a crRNA-4 to integrate the CBE sgRNA expression cassette is additionally highlighted. Black arrows indicate unique ONT reads that cover the entire customized locus. Reads are trimmed as the genome annotation is incomplete (NNN gap highlighted). (**C**) ONT reads were mapped to a customized genome in which we assumed that both cassettes were integrated on the same allele and could be detected on a single ONT read. (**D**) Illumina read coverage was normalized and chromosome coverage was compared to coverage of individual genetic features on these chromosomes.

Figure 4 S2. Sequencing of clones isolated from an AsCas12a-mediated library transfection. *L. mexicana*, *L. major* and *L. donovani* tdTomato/pTB107 cell lines were co-transfected with a library containing a mixtures of 15 guides and Cas12a crRNA-4 targeting the 18S rRNA SSU locus. Library clones from library transfection were isolated and their CBE sgRNA amplified for Sanger sequencing. **(A)** Sanger sequencing trace plots of the library before and 6 days post transfection. The T7 T10 GG promoter, sgRNA target sequence and the beginning of the sgRNA scaffold sequence are highlighted. (**B**) Sanger sequencing trace plots of guide cassettes sequenced from clones. Highlighted in red are clones that maintain more than one sgRNA.

872 **Figure 4 S3. Novel scoring for CBE sgRNA sorting.** Schematic of new CBE scoring matrix. A
873 sgRNA receives the highest score, when the ratio of available cytosines to resulting STOP codons is
874 1:1. Additionally, the final score depends on the number of possible STOP codons and position of
875 cytosines within the editing window (activities indicated above: high, mid and low).

876 **Figure 5 S3. PF16 gene replacement by using CRISPR/AsCas12a ultra.** (**A**) Map of the PF16
877 locus before and after targeting with Cas12a 5' and 3'crRNA positions indicated. The PF16-ORF is
878 replaced with a pTBlast and pTPuro cassette. Primers used for verification of the ORF replacement
879 are highlighted with PCR amplicon length. (**B**) Visualization of PCR amplicons, showing expected
880 products for pTPuro and pTBlast in the ΔPF16 lane and the amplicon of the PF16-ORF in the
881 PARENT lane (*L. mexicana* tdTomato/pTB107 cell line). (**C** and **D**) Sanger sequencing trace plots of
882 amplicons in (**B**), showing sequencing of the upstream region in (**C**) and downstream region in (**D**).
883 Black arrows indicate Cas12a DSBs. (**E**) Violin plot of pooled replicates from motility tracked non-
884 clonal populations, including the ΔPF16 and PARENT cell line. The total percentage of tracked cells
885 showing a velocity of less than 1 µm/s is highlighted. Each population was analysed using a Cramér-
886 von Mises Test to detect any shift in the population distribution towards lower speed. Percentages are
887 marked with an asterisks when that shift was significant (*$p > 0.05$).

888

889 **SUPPLEMENTARY FILES**

890 **Supplementary File 1. Primers used in this study.**

891 **Supplementary File 2. Plasmid maps.** Genbank files of pTB102, pTB104, pTB105, pTB106 and
892 pTB107.

893 **Supplementary File 3. A protocol for AsCas12a-mediated transfection of CBE sgRNA**
894 **expression cassettes.** Step-by-step protocol includes guidelines for PCR amplification of donor DNA
895 and Cas12a crRNA template DNA, as well as preparations for transfection.

896 **Source code 1. Novel scoring for CBE sgRNA sorting.**

897 Source code for CBE sgRNA scoring described above. The updated data sets can be accessed at
898 http://www.leishbaseedit.net/. The source code for the guide scoring has been uploaded to
899 https://github.com/ElisabethMeiser/Collaboration_Beneke_Meiser.

900 **Source data 1. Raw DNA images of Figure 2 S1B and E.** Details as described in Figure 2 S1.

901 **Source data 2. Raw DNA images of Figure 5B.** Details as described in Figure 5.

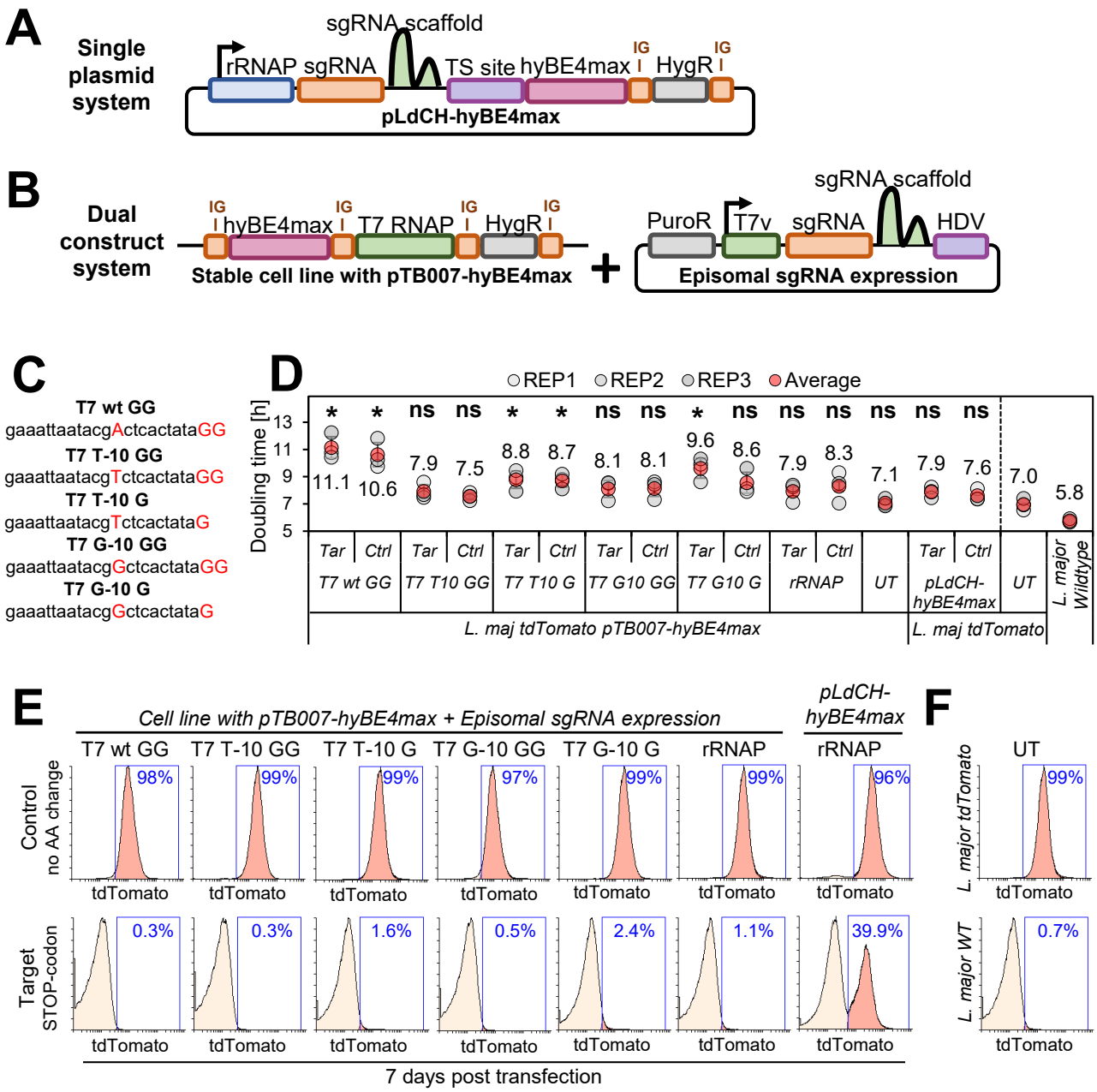
A
Single plasmid system
sgRNA scaffold
rRNAP sgRNA
TS site hyBE4max
IG
HygR
IG
pLdCH-hyBE4max
B
Dual construct system
IG
hyBE4max
IG
T7 RNAP
IG
HygR
IG
Stable cell line with pTB007-hyBE4max
+
sgRNA scaffold
PuroR
T7v
sgRNA
HDV
Episomal sgRNA expression
C
T7 wt GG
gaaattaatacgActcactataGG
T7 T-10 GG
gaaattaatacgTctcactataGG
T7 T-10 G
gaaattaatacgTctcactataG
T7 G-10 GG
gaaattaatacgGctcactataGG
T7 G-10 G
gaaattaatacgGctcactataG
D
REP1
REP2
REP3
Average
Doubling time [h]
13
11
9
7
5
* * ns ns * * ns ns * ns ns ns ns ns ns
11.1 10.6 7.9 7.5 8.8 8.7 8.1 8.1 9.6 8.6 7.9 8.3 7.1 7.9 7.6 7.0 5.8
Tar Ctrl Tar Ctrl Tar Ctrl Tar Ctrl Tar Ctrl Tar Ctrl UT Tar Ctrl UT
T7 wt GG
T7 T10 GG
T7 T10 G
T7 G10 GG
T7 G10 G
rRNAP
UT
pLdCH-hyBE4max
UT
L. major Wildtype
L. maj tdTomato pTB007-hyBE4max
L. maj tdTomato
E
Cell line with pTB007-hyBE4max + Episomal sgRNA expression
pLdCH-hyBE4max
T7 wt GG
T7 T-10 GG
T7 T-10 G
T7 G-10 GG
T7 G-10 G
rRNAP
rRNAP
Control no AA change
98%
99%
99%
97%
99%
99%
96%
Target STOP-codon
0.3%
0.3%
1.6%
0.5%
2.4%
1.1%
39.9%
tdTomato
7 days post transfection
F
UT
L. major tdTomato
99%
L. major WT
0.7%

Figure 1

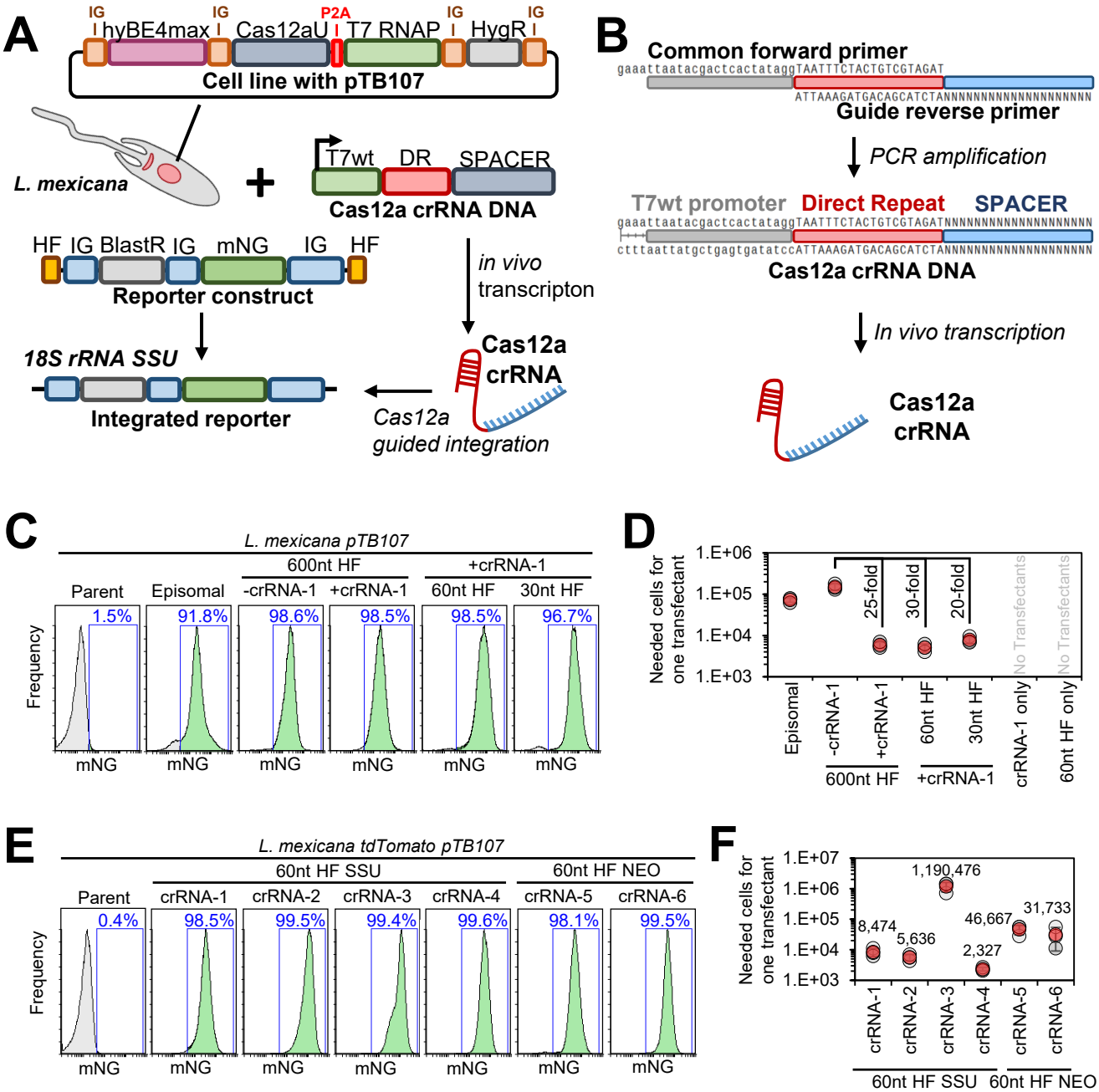
A
IG
hyBE4max
IG
Cas12aU
P2A
T7 RNAP
IG
HygR
IG
Cell line with pTB107
L. mexicana
T7wt
DR
SPACER
Cas12a crRNA DNA
HF IG BlastR IG mNG IG HF
Reporter construct
in vivo transcripton
18S rRNA SSU
Integrated reporter
Cas12a crRNA
Cas12a guided integration
B
Common forward primer
gaaattaatacgactcactataggTAATTTCTACTGTCGTAGAT
ATTAAAGATGACAGCATCTANNNNNNNNNNNNNNNNNNNN
Guide reverse primer
PCR amplification
T7wt promoter
Direct Repeat
SPACER
gaaattaatacgactcactataggTAATTTCTACTGTCGTAGATNNNNNNNNNNNNNNNNNNNN
ctttaattatgctgagtgatatccATTAAAGATGACAGCATCTANNNNNNNNNNNNNNNNNNNN
Cas12a crRNA DNA
In vivo transcription
Cas12a crRNA
C
L. mexicana pTB107
600nt HF
+crRNA-1
Parent
Episomal
-crRNA-1
+crRNA-1
60nt HF
30nt HF
1.5%
91.8%
98.6%
98.5%
98.5%
96.7%
Frequency
mNG
D
Needed cells for one transfectant
1.E+06
1.E+05
1.E+04
1.E+03
25-fold
30-fold
20-fold
No Transfectants
No Transfectants
Episomal
-crRNA-1
+crRNA-1
60nt HF
30nt HF
crRNA-1 only
60nt HF only
600nt HF
+crRNA-1
E
L. mexicana tdTomato pTB107
60nt HF SSU
60nt HF NEO
Parent
crRNA-1
crRNA-2
crRNA-3
crRNA-4
crRNA-5
crRNA-6
0.4%
98.5%
99.5%
99.4%
99.6%
98.1%
99.5%
Frequency
mNG
F
Needed cells for one transfectant
1.E+07
1.E+06
1.E+05
1.E+04
1.E+03
1,190,476
8,474
5,636
2,327
46,667
31,733
crRNA-1
crRNA-2
crRNA-3
crRNA-4
crRNA-5
crRNA-6
60nt HF SSU
60nt HF NEO

Figure 2

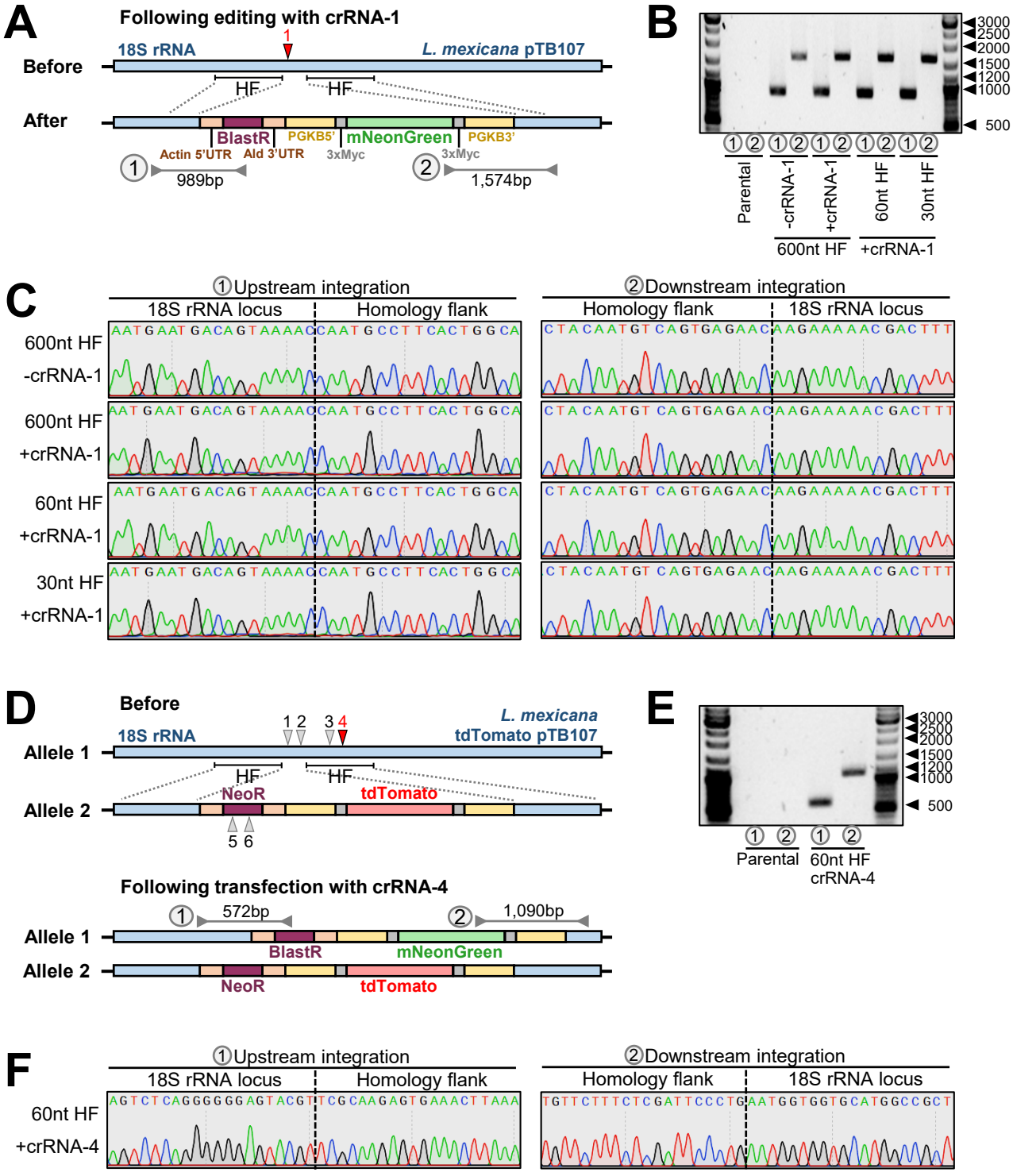
A
Following editing with crRNA-1
18S rRNA
L. mexicana pTB107
Before
After
HF
HF
BlastR
PGKB5'
mNeonGreen
PGKB3'
Actin 5'UTR
Ald 3'UTR
3xMyc
3xMyc
989bp
1,574bp
B
3000
2500
2000
1500
1200
1000
500
Parental
-crRNA-1
+crRNA-1
60nt HF
30nt HF
600nt HF
+crRNA-1
C
①Upstream integration
②Downstream integration
18S rRNA locus
Homology flank
Homology flank
18S rRNA locus
600nt HF
-crRNA-1
600nt HF
+crRNA-1
60nt HF
+crRNA-1
30nt HF
+crRNA-1
D
Before
L. mexicana
tdTomato pTB107
18S rRNA
Allele 1
Allele 2
HF
HF
NeoR
tdTomato
Following transfection with crRNA-4
572bp
1,090bp
Allele 1
Allele 2
BlastR
mNeonGreen
NeoR
tdTomato
E
3000
2500
2000
1500
1200
1000
500
Parental
60nt HF
crRNA-4
F
①Upstream integration
②Downstream integration
18S rRNA locus
Homology flank
Homology flank
18S rRNA locus
60nt HF
+crRNA-4

Figure 2 S1

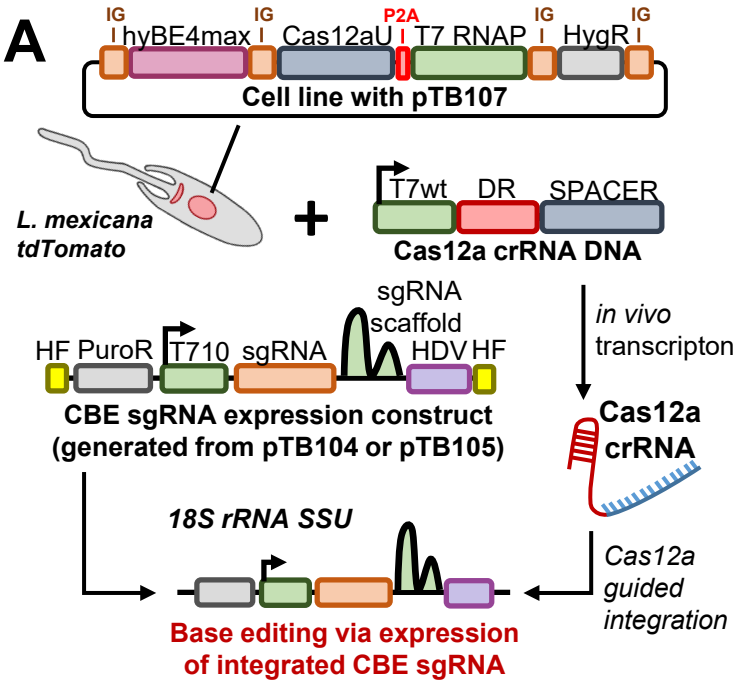
A
IG
hyBE4max
IG
Cas12aU
P2A
T7 RNAP
IG
HygR
IG
Cell line with pTB107
L. mexicana
tdTomato
T7wt
DR
SPACER
Cas12a crRNA DNA
sgRNA
scaffold
HF PuroR
T710
sgRNA
HDV HF
CBE sgRNA expression construct
(generated from pTB104 or pTB105)
in vivo
transcripton
Cas12a
crRNA
18S rRNA SSU
Cas12a
guided
integration
Base editing via expression
of integrated CBE sgRNA

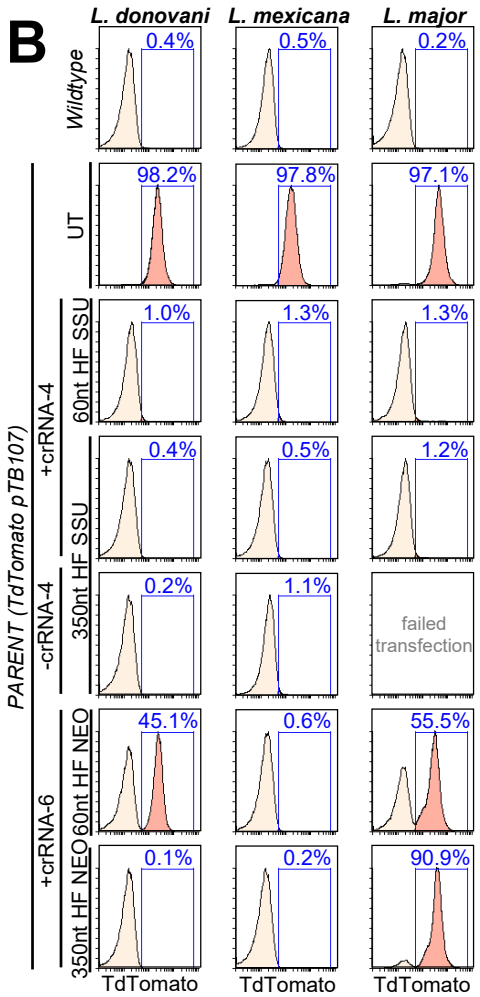
B
L. donovani
L. mexicana
L. major
Wildtype
0.4%
0.5%
0.2%
UT
98.2%
97.8%
97.1%
+crRNA-4
60nt HF SSU
1.0%
1.3%
1.3%
350nt HF SSU
0.4%
0.5%
1.2%
-crRNA-4
350nt HF SSU
0.2%
1.1%
failed
transfection
+crRNA-6
60nt HF NEO
45.1%
0.6%
55.5%
350nt HF NEO
0.1%
0.2%
90.9%
PARENT (TdTomato pTB107)
TdTomato
TdTomato
TdTomato

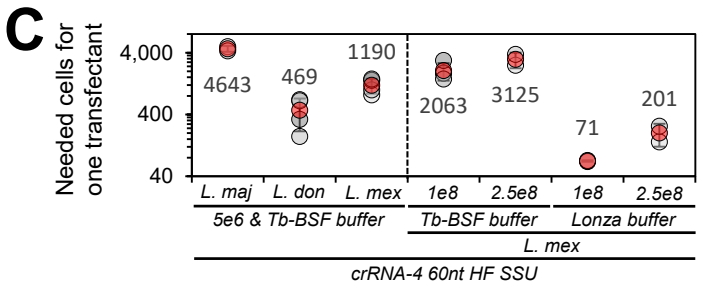
C
Needed cells for
one transfectant
4,000
400
40
4643
469
1190
2063
3125
71
201
L. maj
L. don
L. mex
1e8
2.5e8
1e8
2.5e8
5e6 & Tb-BSF buffer
Tb-BSF buffer
Lonza buffer
L. mex
crRNA-4 60nt HF SSU

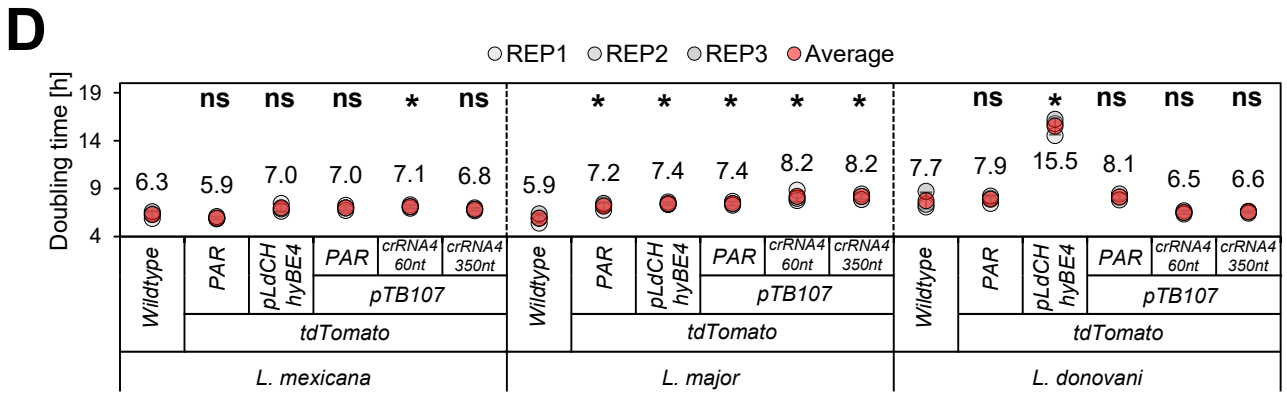
D
REP1
REP2
REP3
Average
Doubling time [h]
19
14
9
4
ns
ns
ns
*
ns
6.3
5.9
7.0
7.0
7.1
6.8
*
*
*
*
*
5.9
7.2
7.4
7.4
8.2
8.2
ns
*
ns
ns
ns
7.7
7.9
15.5
8.1
6.5
6.6
Wildtype
PAR
pLdCH hyBE4
PAR
crRNA4 60nt
crRNA4 350nt
pTB107
tdTomato
L. mexicana
L. major
L. donovani

Figure 3

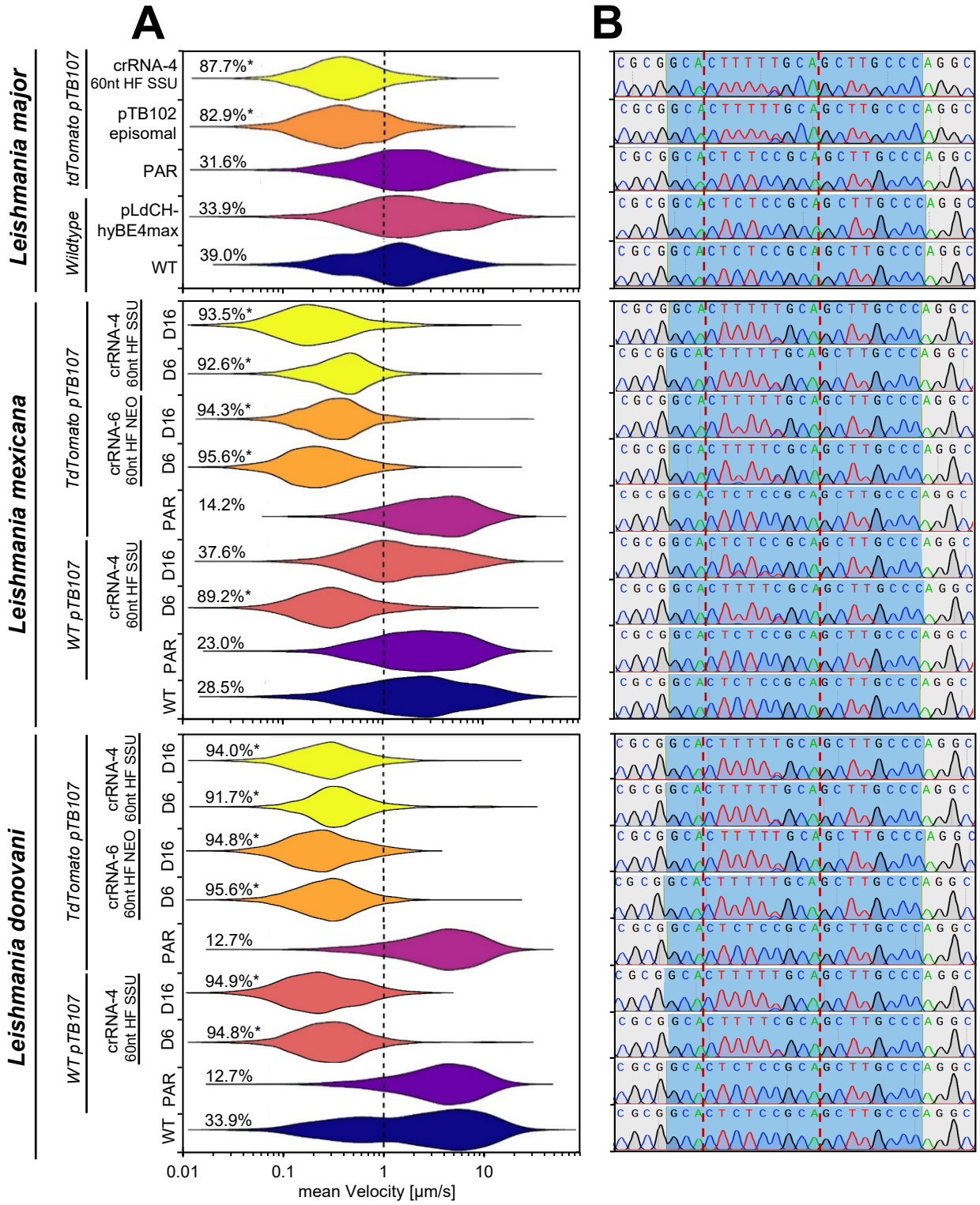
A
B
Leishmania major
tdTomato pTB107
Wildtype
crRNA-4
60nt HF SSU
pTB102
episomal
PAR
pLdCH-
hyBE4max
WT
87.7%*
82.9%*
31.6%
33.9%
39.0%
Leishmania mexicana
TdTomato pTB107
WT pTB107
crRNA-4
60nt HF SSU
crRNA-6
60nt HF NEO
D16
D6
PAR
WT
93.5%*
92.6%*
94.3%*
95.6%*
14.2%
37.6%
89.2%*
23.0%
28.5%
Leishmania donovani
94.0%*
91.7%*
94.8%*
95.6%*
12.7%
94.9%*
94.8%*
12.7%
33.9%
0.01
0.1
1
10
mean Velocity [µm/s]

Figure 4

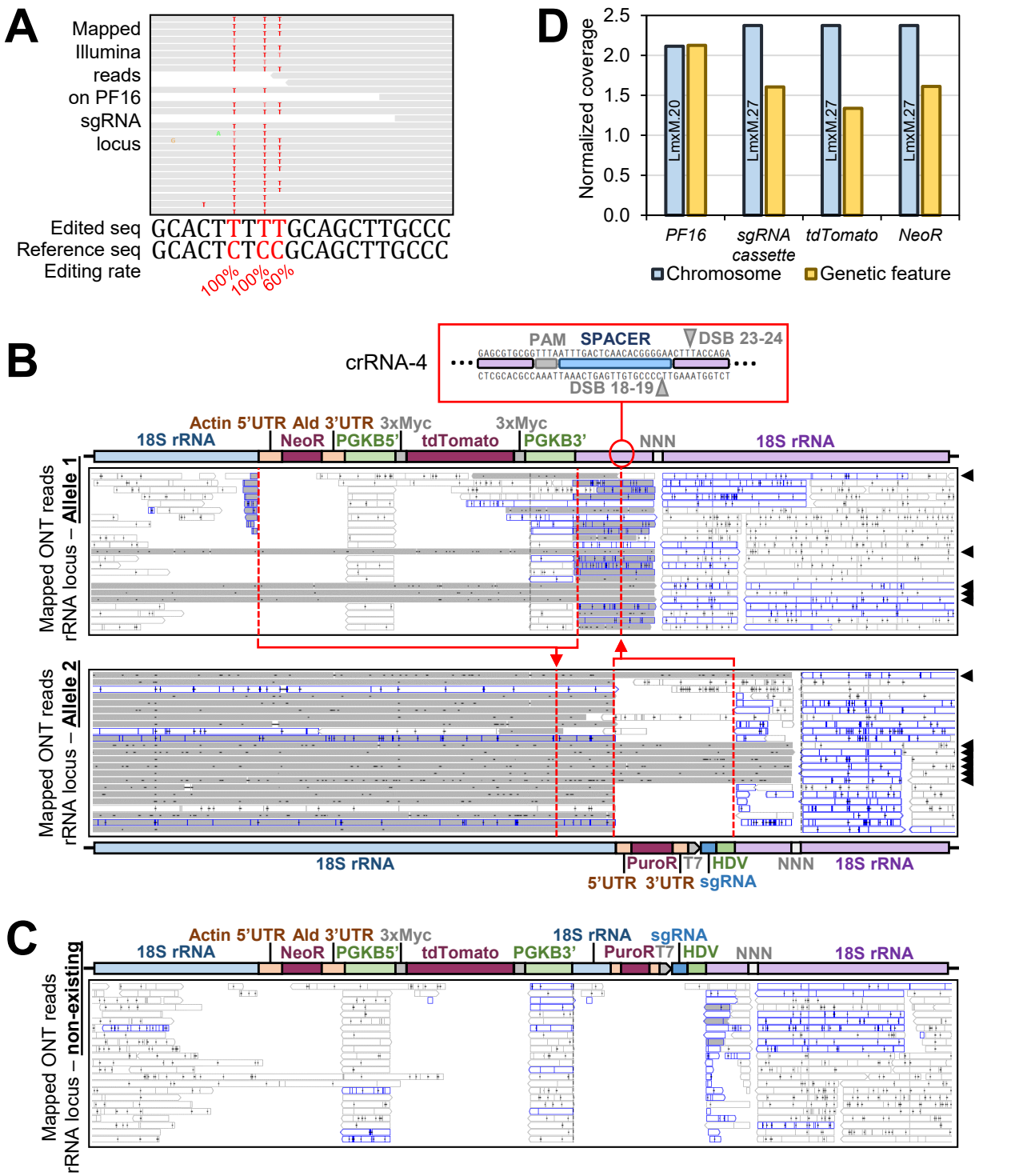
A
Mapped Illumina reads on PF16 sgRNA locus
Edited seq GCACTTTTTGCAGCTTGCCC
Reference seq GCACTCTCCGCAGCTTGCCC
Editing rate
100% 100% 60%
D
Normalized coverage
2.5
2.0
1.5
1.0
0.5
0.0
LmxM.20
LmxM.27
LmxM.27
LmxM.27
PF16
sgRNA cassette
tdTomato
NeoR
Chromosome
Genetic feature
B
crRNA-4
PAM
SPACER
DSB 23-24
DSB 18-19
Actin 5'UTR
Ald 3'UTR
3xMyc
3xMyc
18S rRNA
NeoR
PGKB5'
tdTomato
PGKB3'
NNN
18S rRNA
Mapped ONT reads rRNA locus – Allele 1
Mapped ONT reads rRNA locus – Allele 2
18S rRNA
PuroR
T7
HDV
NNN
18S rRNA
5'UTR
3'UTR
sgRNA
C
Mapped ONT reads rRNA locus – non-existing
Actin 5'UTR
Ald 3'UTR
3xMyc
18S rRNA
sgRNA
18S rRNA
NeoR
PGKB5'
tdTomato
PGKB3'
PuroR
T7
HDV
NNN
18S rRNA

Figure 4 S1

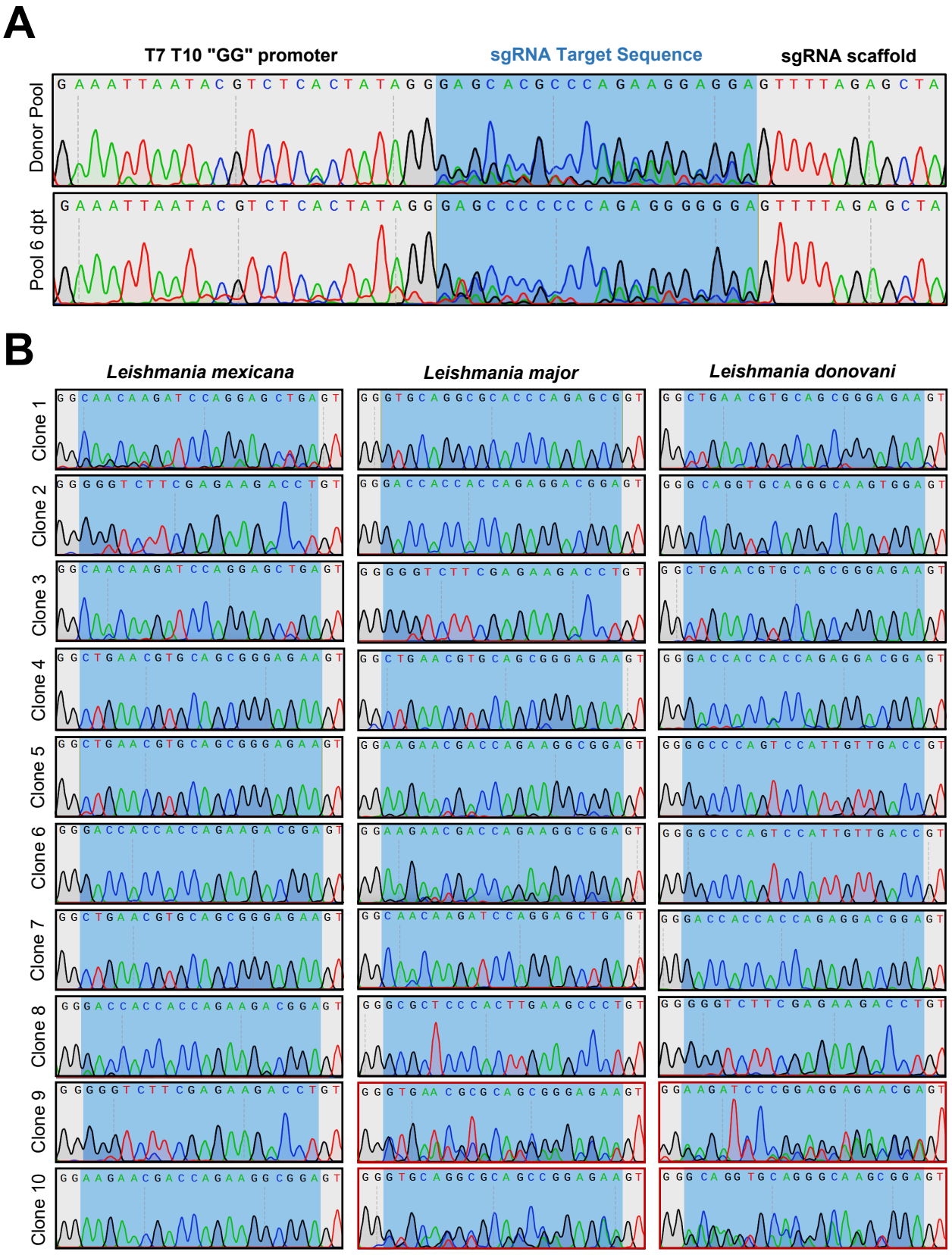
A
T7 T10 "GG" promoter
sgRNA Target Sequence
sgRNA scaffold
Donor Pool
Pool 6 dpt
B
Leishmania mexicana
Leishmania major
Leishmania donovani
Clone 1
Clone 2
Clone 3
Clone 4
Clone 5
Clone 6
Clone 7
Clone 8
Clone 9
Clone 10

Figure 4 S2

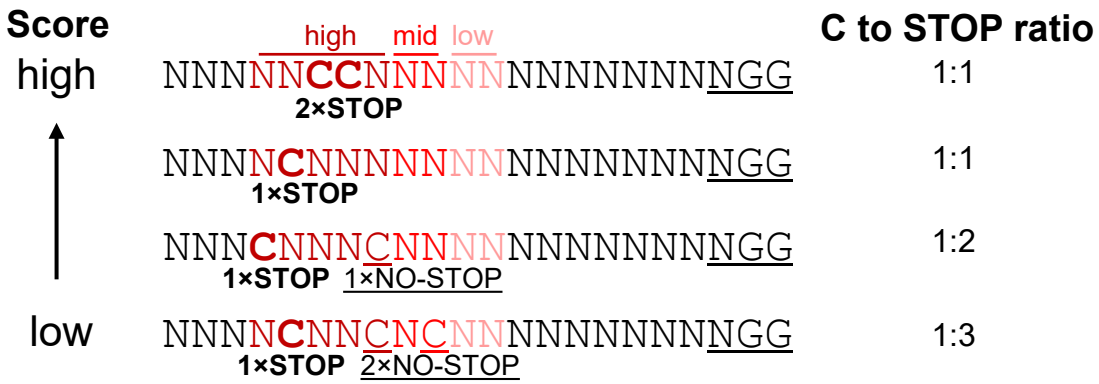
Score
high
low
high
mid
low
C to STOP ratio
NNNNNCCNNNNNNNNNNNNNNNGG
2×STOP
1:1
NNNNCNNNNNNNNNNNNNNNNGG
1×STOP
1:1
NNNCNNNCNNNNNNNNNNNNNGG
1×STOP
1×NO-STOP
1:2
NNNNCNNCNCNNNNNNNNNNNGG
1×STOP
2×NO-STOP
1:3

Figure 4 S3

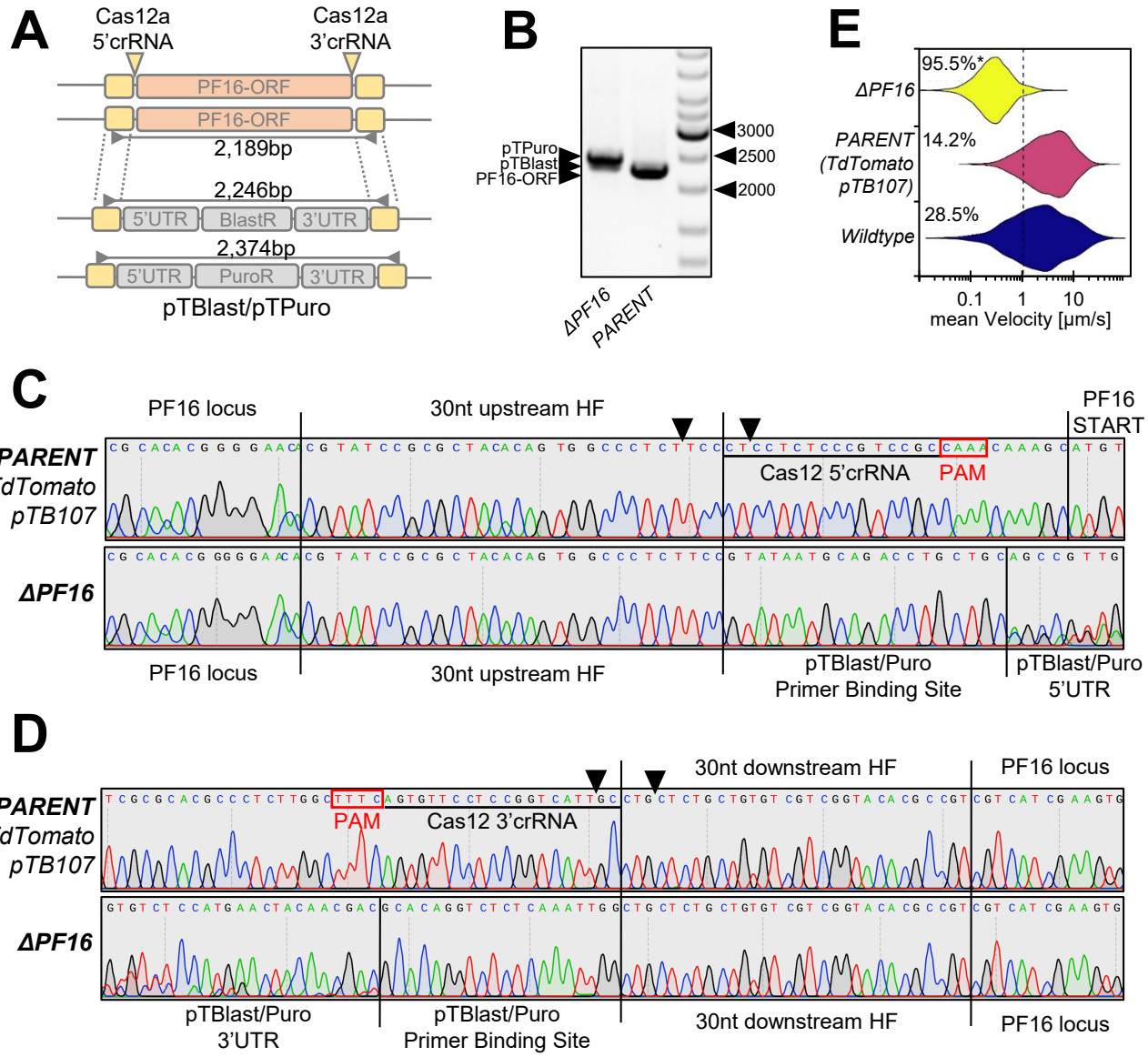
A
Cas12a
5'crRNA
Cas12a
3'crRNA
PF16-ORF
PF16-ORF
2,189bp
2,246bp
5'UTR
BlastR
3'UTR
2,374bp
5'UTR
PuroR
3'UTR
pTBlast/pTPuro
B
pTPuro
pTBlast
PF16-ORF
3000
2500
2000
ΔPF16
PARENT
E
95.5%*
ΔPF16
PARENT
(TdTomato
pTB107)
14.2%
28.5%
Wildtype
0.1
1
10
mean Velocity [µm/s]
C
PF16 locus
30nt upstream HF
PF16
START
PARENT
TdTomato
pTB107
Cas12 5'crRNA
PAM
ΔPF16
PF16 locus
30nt upstream HF
pTBlast/Puro
Primer Binding Site
pTBlast/Puro
5'UTR
D
30nt downstream HF
PF16 locus
PARENT
TdTomato
pTB107
PAM
Cas12 3'crRNA
ΔPF16
pTBlast/Puro
3'UTR
pTBlast/Puro
Primer Binding Site
30nt downstream HF
PF16 locus

Figure 5